Evidences for a Noachian–Hesperian orogeny in Mars

Francisco Anguita , Carlos Fernández , Guadalupe Cordero , Sandra Carrasquilla , Jorge Anguita , Andrés Núñez , Sergio Rodríguez , Judit García

Abstract

A number of tectonic structures have been located at the Thaumasia Plateau, Daedalia Planum and Aonia Terra, Mars. They include isolated folds with axial traces up to 200 km long, trains of tightly folded structures tens of km long, and thrusts. Their size and geometry are similar to those on Earth, and the direction of compression seems to have varied amply with time, suggesting a complex tectonic evolution. Crater counts on the deformed terrain point to Noachian to Early Hesperian ages. On the basis of the geometry and geological relations of these structures, we propose that they form part of an old martian orogen, the Thaumasia–Aonia Orogen, which embraced not only the Thaumasia Plateau, but areas of Daedalia Planum, Aonia Terra and Nereidum Montes as well. A regional coherent layering is previous to the deformation and could represent the trace of even older stresses on the martian lithosphere.

Keywords: Mars; Geological processes; Tectonics

1. Introduction

As is true for Archaean Earth, Mars Noachian times (4.6 to 3.7/3.5 Gyr; Hartmann and Neukum, 2001) is the critical epoch in planetary formation. This is a time when a powerful geodynamo was in action and when most of the crust was produced. It is also a time where two of the great controversies of the present Planetary Sciences (are there life, and plate tectonics, beyond the Earth?) could be elucidated. The unknowns over this billion-year long period are impressive: the abundance (and possible massive loss) of volatiles, the initial climate, the mechanisms of crust formation, or the inception of the Tharsis bulge and the structural influence it had on the rest of the planet. The first reference to plate tectonics in Mars is due to Sengör and Jones (1975), but it was not until the controversial work of Sleep (1994) that the possible recycling of the martian lithosphere began to rank high among the former questions. This author emphasized that "structural relations from photogeology are the data most likely to test and modify hypotheses about Mars plate tectonics." In this paper we present the results of a critical revision of images which show that in Noachian times Mars experienced tectonic processes amounting, in range and intensity, to what in Earth geology we would term an orogeny.

Spagnuolo and Dohm (2004) have been the first authors to use the word orogeny for Mars, though the associated expressions "mountain ranges" and "mountain building" have been introduced in descriptions (Scott and Tanaka, 1981; Dohm et al., 2002; Baker et al., 2005) of the reliefs of at least an area peripheral to Tharsis province: the Thaumasia Highlands. It is also true that the authors (Connerney et al., 1999; Nimmo and Stevenson, 2000; Zhong and Zuber, 2001; Hauberg and Kronberg, 2001; Fairén et al., 2002; Baker et al., 2002; Dohm et al., 2002; Fairén and Dohm, 2004) that have defended some form of martian plate tectonics theory are implicitly sustaining the existence of structural belts similar (?) to Earth mountain chains. Up to the present, notwithstanding, Thar-

sis tectonic structures have been systematically interpreted as a side effect of the uplift of the dome. We present here new evidence for these structures to be unrelated to the Tharsis bulge influence, and therefore we conclude that they are due to deviatoric stresses with horizontal maximum compressive axis which operated in various directions and at different times, thus attesting to a complex structural history for Mars. We do not state that we are proving martian plate tectonics; the importance of the evidence presented requires, however, an explanation that, given the Noachian age of most structures, should be taken into account in the current discussion on the first martian dynamic regime.

2. The Thaumasia Plateau and neighboring plains

The Thaumasia region (Plescia and Saunders, 1982; Schultz and Tanaka, 1994; Tanaka et al., 1998; Dohm and Tanaka, 1999) is the southern part of the Tharsis volcanotectonic province (Fig. 1). It includes the Thaumasia Plateau, a roughly semicircular highland 2900 km across bound by Valles Marineris and by a range (the Thaumasia and Coprates highlands, Claritas and Nectaris Fossae) which rises more than 4 km over the neighboring plains. A number of old volcanic constructs have been identified at Thaumasia and Daedalia Planum (Dohm and Tanaka, 1999), and the outcropping materials are probably basaltic types (Bandfield et al., 2000). Mars Global Surveyor (MGS) gravity survey has defined a neat positive free-air gravity anomaly under Thaumasia Highlands and Claritas Fossae, paralleled by a negative anomaly ring at the foot of the highlands (Zuber et al., 2000).

The tectonic structures in the plateau include Claritas Fossae, one of the oldest and longest sets of grabens in Tharsis, as well as strike-slip faults and compressive structures such as buckling, folds and thrusts. Many of these structures have been intensely studied by Plescia and Saunders (1982), Schultz and Tanaka (1994), Tanaka et al. (1998), Dohm and Tanaka (1999), Phillips et al. (2001), Anderson et al. (2001), Anguita et al. (2001), Anderson et al. (2004), Fairén and Dohm (2004), and Johnson and Phillips (2005). There is now a consensus that the plateau has been thrusted over the neighboring plains; this has nevertheless been attributed to different causes. Dohm and Tanaka (1999) suggested that the intrusion of low-density materials caused uplift, with grabens in the middle and folded and thrusted margins. Webb and Head (2001, 2002) propose a mega-slide from the Syria Planum volcanic center, with thrusting borders at Coprates and Thaumasia Highlands, and Fairén and Dohm (2004) put forward the hypothesis that the Thaumasia Plateau is the martian equivalent of Earth intracontinental igneous plateaux like the Deccan Traps.

While the Thaumasia Plateau is neatly defined as a geographical unit, its geological limits are less certain. Schultz and Tanaka (1994), and more recently Okubo and Schultz (2004), suggest that the plateau could be a part of a larger geologic realm, the South Tharsis Ridge Belt, defined by large rises which they interpret as contractional structures. This broader area includes parts of two neighboring provinces: Daedalia Planum to the west and Aonia Terra to the east (Fig. 1). Daedalia Planum, suggested by Craddock et al. (1990) as an ancient impact basin, is a regional plain surrounded by ridges that are surface expressions of sinistral strike-slip faults (Anguita et al., 2001). As an example, Gordii Dorsum (2–8° N, 142–146° W) has been proven to have a 30 to 40 km sinistral slip (Forsythe and Zimbelman, 1988). Aonia Terra is a heavily cratered region that includes a number of ridges (see Section 3, Zone H) such as Bosporos Rupes, Ogygis Rupes and the unnamed scarps centered at 37° S 60° W, 45° S 67° W, or 50° S 68° W. Bosporos Rupes, the most prominent of them, is a 600 km-long ridge that deforms Nereidum Montes, a part of the ring-shaped terrain uplifted and fractured by the Argyre impact. Thus, at least Bosporos Rupes was demonstrably produced later than this giant impact.

This deduction has a bearing on the age of the deformation of the Thaumasia Plateau. On the basis of their crater counts, the surface geological units of the plateau (Scott and Tanaka, 1986) are dated as Noachian to Hesperian (3.7/3.5 to ~3 Gyr; Hartmann and Neukum, 2001). Lower Noachian terrains, the oldest outcropping martian basement, are widespread throughout Thaumasia (Scott and Dohm, 1990). To confirm these ages, crater counts have been carried out at four areas considered representative: the Zones C, D, F, and I (Fig. 1, Appendix A), the first three at the western, southern, and eastern plateau borders, and the last one at the best defined of the outer structural zones. Since crater counts in very old martian surfaces are nevertheless subjected to important statistical errors, the age of the belt can be deduced only with a degree of uncertainty: not earlier than ~4.0 Gyr (the median age of the great impact basins), and not later than ~3.0 Gyr (the youngest well defined isochron, see Section 3, Zone C). Taking in account the rapid decline of the impact rates between 4.0 and 3.4 Gyr, Hartmann and Neukum (2001) justify the difficulty of building precise isochrons for this period. This notwithstanding, the curves obtained adjust approximately to the steady state line defined by Hartmann and Neukum (2001). The curves show a systematic decrease in crater numbers between 16 and 0.5 km diameter craters, a fact traceable to an epoch of increased erosion. All surfaces measured give ages older than 3.0 Gyr for crater sizes larger than 0.2 km.

3. Structural analyses

We have selected (Fig. 1) six areas (Zones A to F) of the Thaumasia Plateau for our structural analyses, including also three additional regions at the borders of Daedalia Planum, at Aonia Terra and at Nereidum Montes (Zones G to I), which share structural features with Thaumasia. Simplified versions of the geologic map by Dohm et al. (2001) have been reproduced in order to put in a geologic context the tectonic structures.

Zone A (Fig. 2) is centered at 19° S 108° W, at the northwestern end of Thaumasia Highlands. The MOC image and its interpretation (Figs. 2a and 2b) allow to map the basement layering (Nb), partly covered by units defined as Hesperian (Hf). The Viking frame and the geological mapping (Figs. 2c and 2d) give the context. These mapped structures are comparable to some fold-and-thrust belts on Earth, as found, for example,

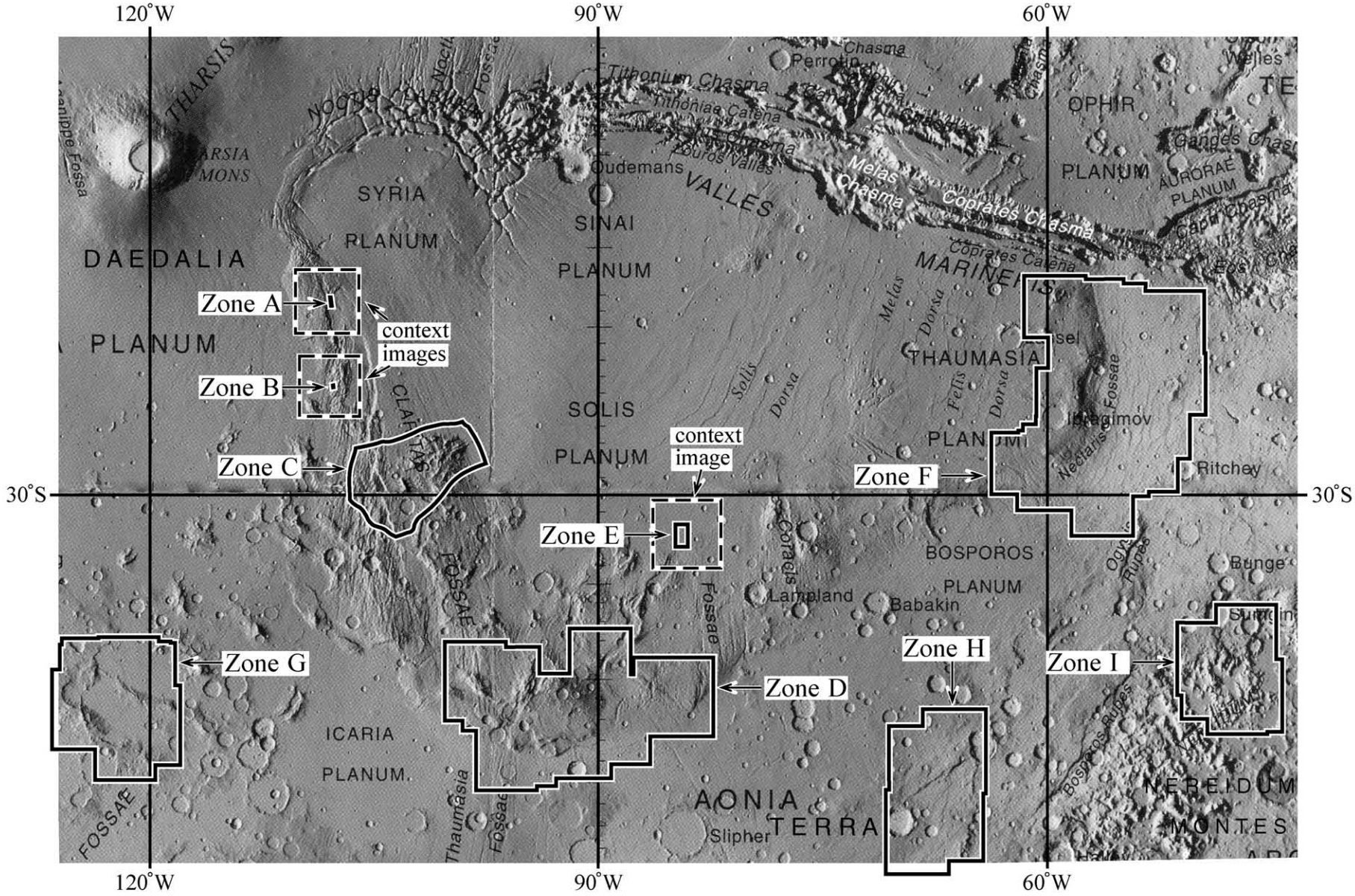

Fig. 1. Map of the studied area, covering the Thaumasia Plateau, Daedalia Planum and Aonia Terra. Figs. 2–10 are indicated.

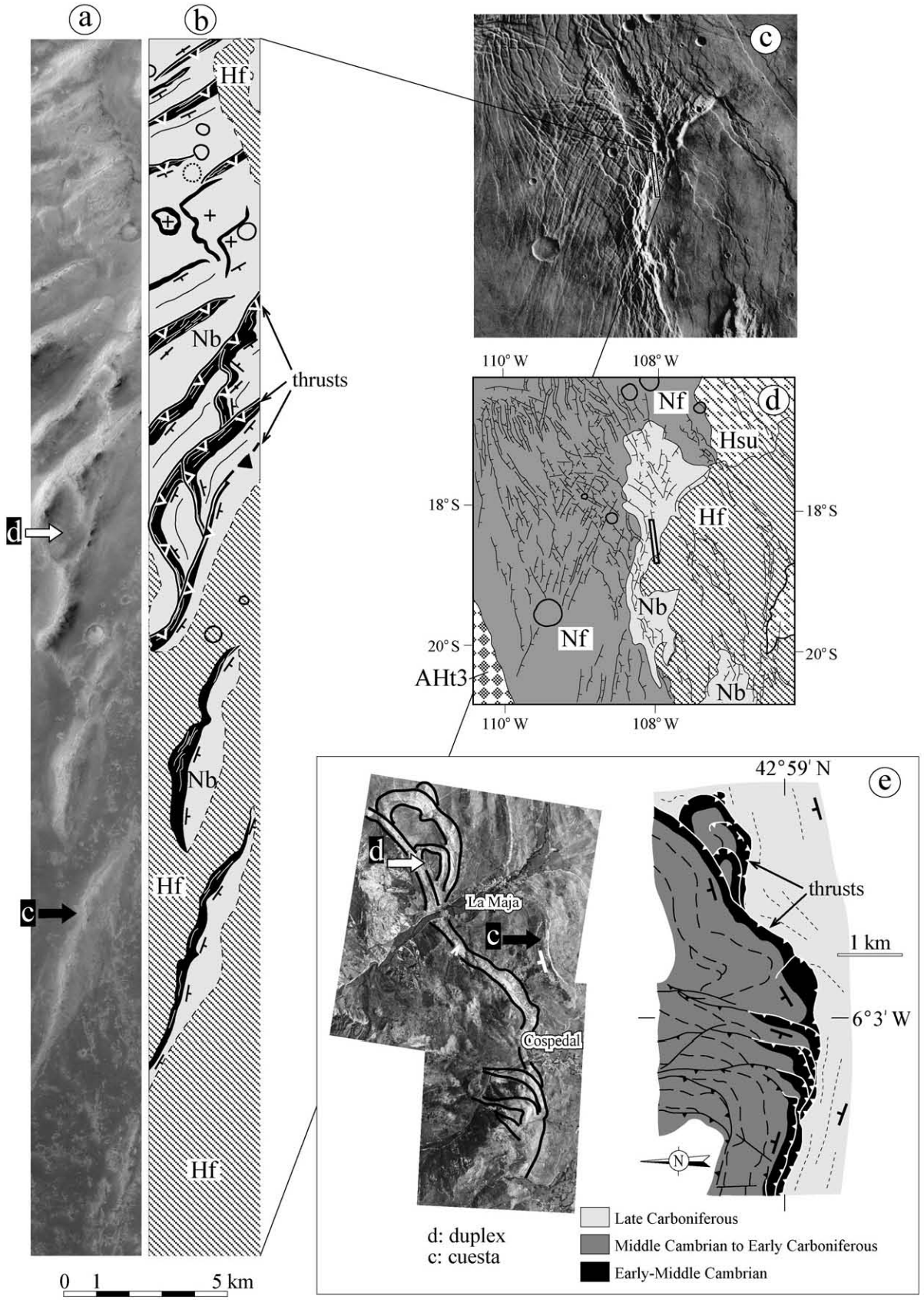

Fig. 2. Zone A (see Fig. 1 for location). (a) MOC image m1300830. (b) Structural map of the Nb unit. (c) Reference frame. (d) General geological map modified from Dohm et al. (2001). (e) Aerial photograph and geological map (modified from Suárez et al., 1991) of a similar area of the Variscan Iberian Massif.

at the Iberian Massif, Spain (Pérez Estaún et al., 1988). The area portrayed in Fig. 2e represents the foreland fold-and-thrust belt of the Variscan orogen, a thin-skinned structure composed of a set of imbricate thrusts, fans, duplexes and geometrically related folds, with cuestas formed through the erosion of the thrusts. Patterns similar to all these morpho-structures can be observed in Zone A (Figs. 2a and 2b).

Hauber and Kronberg (2003, 2005) have described important extensional structures in the Thaumasia Graben, which includes our Zone A located at the northwestern part of this graben. However, the following arguments strongly dismiss the extensional hypothesis for the structures observed in Zone A. Firstly, extension in the Thaumasia Graben is Late Hesperian–Early Amazonian (Hauber and Kronberg, 2003, 2005), which is younger than the structures we describe here in Zone A. Secondly, the strike of the extensional faults in the northern Thaumasia Graben is 20°–30° W, differing from the 10°–40° E azimuth of the structures in Zone A (Fig. 2). Thirdly, the geometry of duplexes and sinuous structures mapped in Zone A (Fig. 2b) is typical of contractional regimes and more difficult to observe in extensional settings. Although we cannot completely discard the extensional hypothesis for our described features, we rather prefer the contractional explanation of these structures as thrusts, according to the previous arguments. A point to be stressed is that the direction of these thrusts is by no means concentric to Tharsis, which contradicts the widely held view after which compressional structures on and around the dome are due to its flexural loading. For instance, Banerdt and Golombek (2000) propose that most tectonic structures in the western hemisphere of Mars are consistent with a state of flexural support for Tharsis, while Mueller and Golombek (2004) argue that the Tharsis' wrinkle ridges were produced by flexural loading of the martian lithosphere.

Zone B is centered at 22° S 108° W, in the northwestern Thaumasia Highlands (Fig. 3). The Noachian basement unit (Nb) displays a ~10° E-trending layering that appears to be deeply eroded. The exposure morphology indicates that the layers consistently dip towards the west (Figs. 3a and 3b). This area, although small, seems representative of most of the zone shown in Fig. 3c. Areas with west and east dipping layering alternate with each other, thus defining a train of northerly-trending folds. More examples of such structures will be seen at Zone E.

Zone C, centered at 28° S 103° W, is located at western Thaumasia Highlands (Fig. 4). The most relevant structural feature (Fig. 4a) for this region is a 200 km antiformal fold (Figs. 4b and 4c) with an E–W-directed axial trace. This antiformal fold belongs to the basement complex (Nb) and plunges under younger Noachian (Nf) units. Both of these units show a conspicuous, though enigmatic, layering, which could represent an igneous, metamorphic or deformation banding. At the eastern part of the area the strike of this layering is E–W, with a consistent dip to the N (Fig. 4a). The layering is also affected by other E–W-trending folds of variable but always important wavelength (from 10 to 50 km, e.g., at 28° S 102° W, Figs. 4a and 4b). These folds control the shape of the contact between Nb and Nf, which includes several prominent periclinal closures (white arrows in Fig. 4a). Westward and eastward-dipping closures are evidence of sinuous fold hinges. Indeed, the intricate geometry of the Nb–Nf contact is indicative of fold interference structures. A second set of large, NW–SE-trending, open folds have been identified at, for instance, 29° S 100° W, where they bend the axial plane of the E–W folds. The resulting, highly complex geometry follows patterns intermediate between the types 1 and 2 of the classical models of Ramsay (1967). An example (Figs. 4b and 4c, marked with a black arrow in Fig. 4a) exhibits the geometry of modified Type 1 interference folds (Fig. 4d; Ghosh et al., 1992; Simón, 2004). The structural analysis of this zone reveals still another stage of folding, which affected the Nf and HNf units with small-wavelength folds (arrow with oblique pattern in Fig. 4a), whose tips abut against one of the interference forms. The resulting geometry is very similar to that of the snake-like folds defined by Simón (2005) which represent a case of an erosion-controlled tectonic structure (Fig. 4e). Removal of the overburden allowed the eastern limb of the large N–S folds in Fig. 5e (martian and terrestrial cases) to behave as independent layers and to become locally refolded into minor folds showing a snake-like map geometry. An important period of erosion took therefore place before the HNf unit deposition.

In all, a sequence of three fold generations is observed in this area: the first two folding stages, which produced the large folds and interference patterns, were previous to the deposition of the HNf (Noachian–Hesperian) unit, so they can therefore be confidently dated as Noachian. A third generation, with smaller folds, seems to mark the waning stages of the deformation history. As indicated by the crater counts (Fig. 4f), these deformation episodes affected this region until at least the earliest Hesperian times. The presence at Solis Dorsa, some 1000 km eastwards, of wrinkle ridges of Amazonian age (e.g., Anguita et al., 2001) means that further compressional stresses affected this area; nevertheless, the absence of Amazonian outcrops makes difficult to evaluate their effects.

Zone D is centered at 43° S 96° W, in the region called Warrego Valles, the southernmost point of Thaumasia Highlands (Figs. 5a and 5b). Two types of structures, compressive and extensional, are featured at this area. Compressive structures include lobate scarps and wrinkle ridges, and extensional structures include normal faults and grabens. Some of the lobate scarps (such as for instance those with white arrows in Fig. 5c) mark the limit between the basement and cover terrains. Basement units always form the top of the scarps. The layering of the basement units, approximately parallel to the scarps, dips markedly to the south (Fig. 5c). The oldest cover units (Noachian–Hesperian) dip also to the south, though with a lesser angle. Basement and cover are crossed by lobate scarps and wrinkle ridges (Fig. 5c). Ridge forelimbs primarily appear on the southern side of the structures, although the opposite geometry is also encountered, as are wrinkle ridges with scarps on both faces. Normal faults and grabens cut across most of the compressive structures (Fig. 5d). Up to three graben sets can be distinguished: 10° E, 35° W, and 70° W, in order of decreasing age.

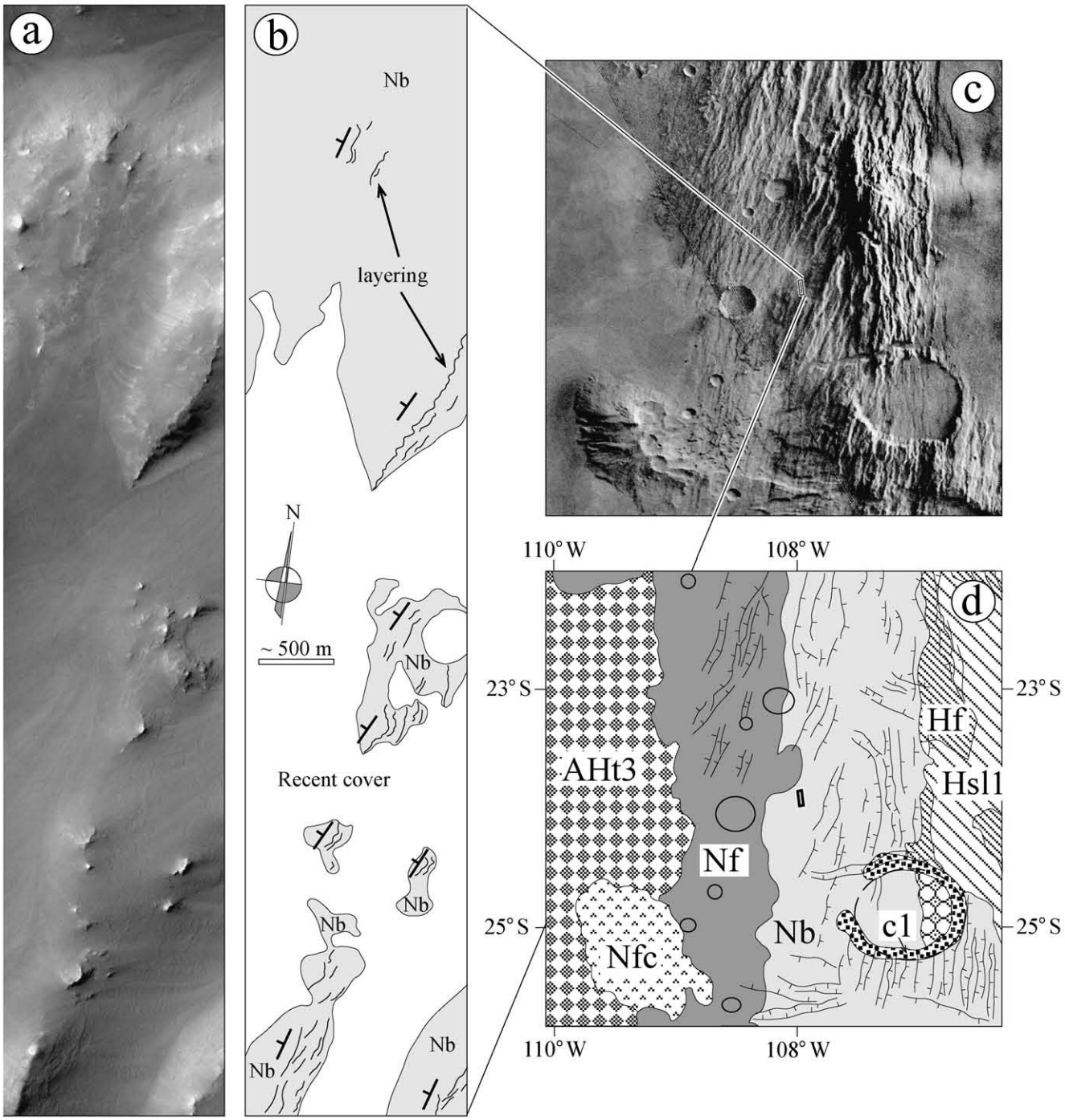

Fig. 3. Mosaic and structural interpretation of Zone B. (a) MOC image m0203644. (b) Geological interpretation of (a). (c) Context image with location of the studied MOC image. (d) Geological map of the area covered by the Viking image, modified from Dohm et al. (2001). Nomenclature of geologic units according to Dohm and Tanaka (1999).

Zone D is covered by a dense, dendritic drainage system (Fig. 5e). The main channels present a centrifugal geometry, radiating from a topographic high around 41° S 92° W. Secondary channels follow the cover materials maximum dip (compare Figs. 5c and 5e), while main channels are oriented parallel to the scarps with a more marked topographic signature. The channels debouch through the relay structures, thus highlighting the drainage structural control. Tanaka et al. (1998) contend that this dense valley network was not carved by rains, but by hydrothermal circulation. If this was the case, it can be concluded that the main fractures acted as preferred conduits for water flow. The crater count curve (Fig. 5f) shows a less marked decrease in the 0.25 to 1 km bins, though always straddling the Noachian–Hesperian time limit.

Lobate scarps are considered by most authors (e.g., Mueller and Golombek, 2004) as thrust fronts of the Noachian basement. Indeed, the systematic presence of Noachian basement at the northern, uplifted sides of the lobate scarps in Warrego

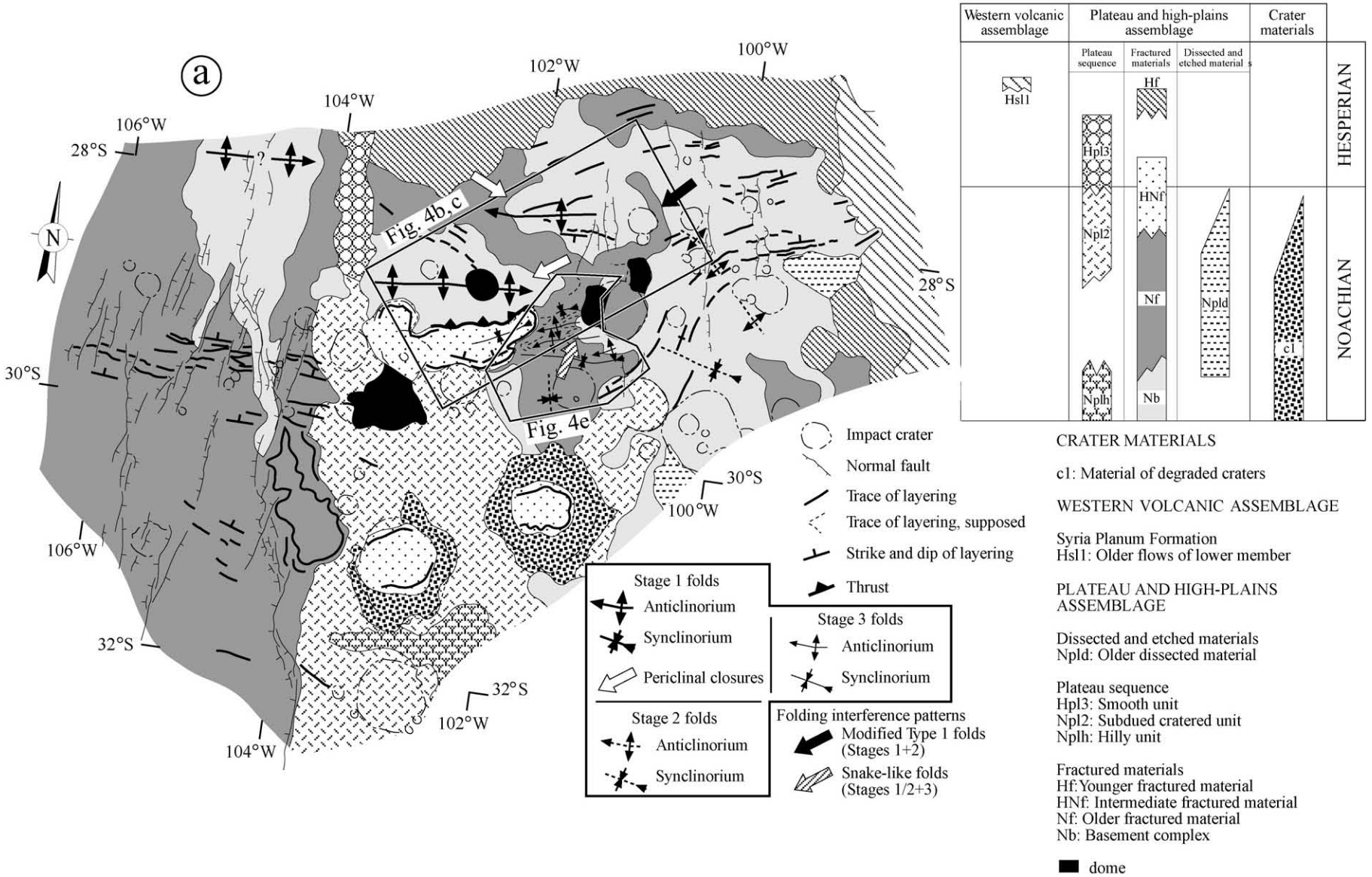

Fig. 4. (a) Structural map of Zone C. Geological map modified from Dohm et al. (2001), and nomenclature of geologic units according to Dohm and Tanaka (1999). (b) Part of the Viking frame 643A42, 102°–104° W, 29° S. (c) Geological interpretation. (d) A modified Type 1 interference fold, a terrestrial analog for the superposed folding structures in (b), from the Iberian Chains of Central Spain (modified from Simón, 2004, 2005). (e) Snake-like folds from the Spain Iberian Chains (modified from Simón, 2004, 2005), and its comparison with similar structures in the central part of Zone C. (f) Crater counts. All craters >1 km are over the 3 Gyr isochron. The depression of the crater count curves between 1 and 10 km crater diameters for Noachian terrains has been remarked by Hartmann and Neukum (2001).

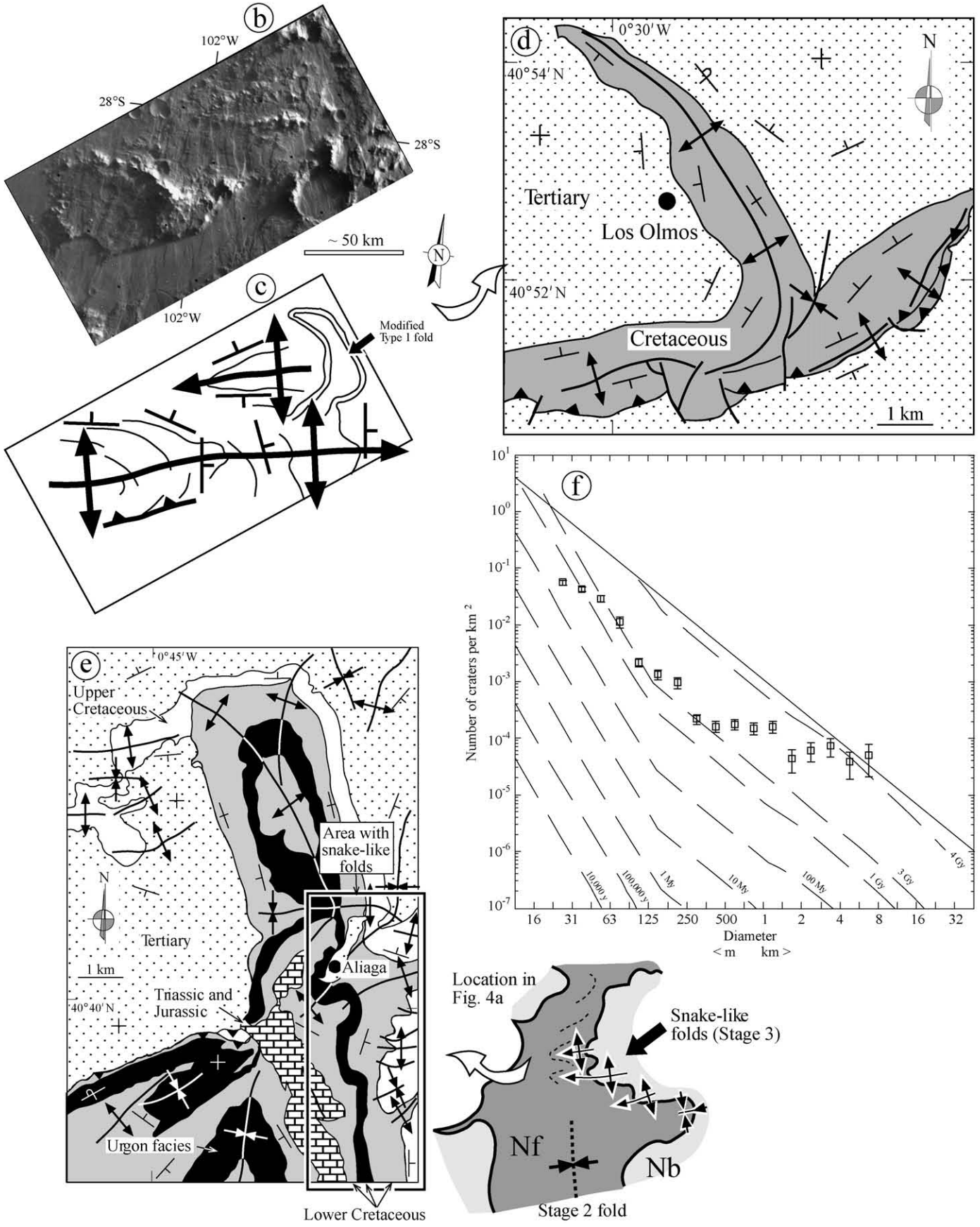

Fig. 4. (*continued*)

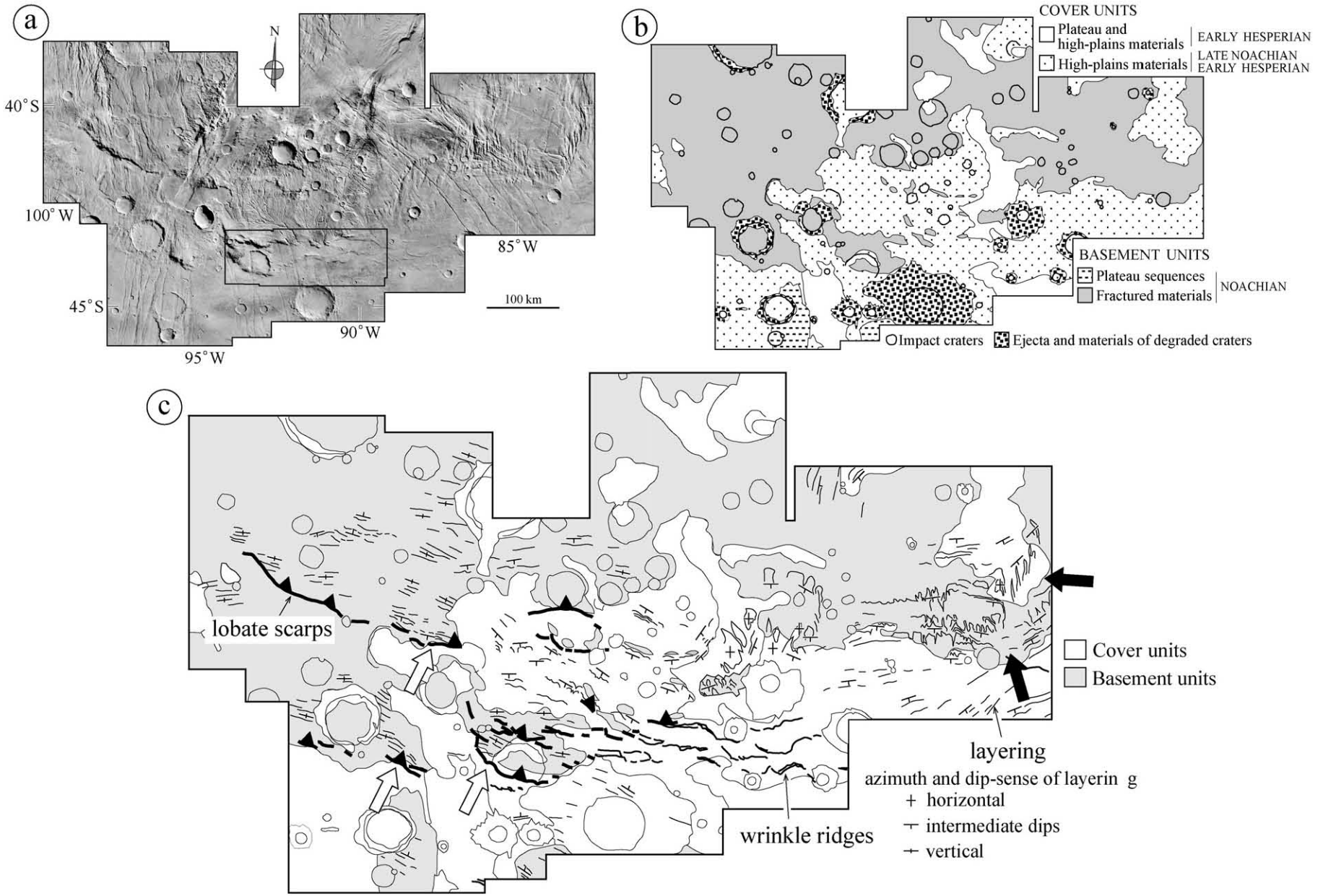

Fig. 5. Mosaic (a) and geologic map [(b), modified from Dohm et al., 2001] of Zone D, Warrego Valles. (c) Structural interpretation of compressive structures. White arrows indicate zones where lobate scarps mark the limit between basement and cover. Black arrows indicate a marked convex-southward curvature of layering. (d) Normal faults and grabens. (e) Drainage pattern. (f) Crater count curve. (g) Mosaic, structural interpretation and ideal schematic cross section of the area outlined at center of (a). Arrows with an oblique pattern mark en echelon layout of lobate scarps and wrinkle ridges. Small gray arrow indicates the area with lateral transition between lobate scarps and wrinkle ridges. (h) An analog at the Alpine Cantabrian belt, northern Spain (modified from Alonso and Pulgar, 2004).

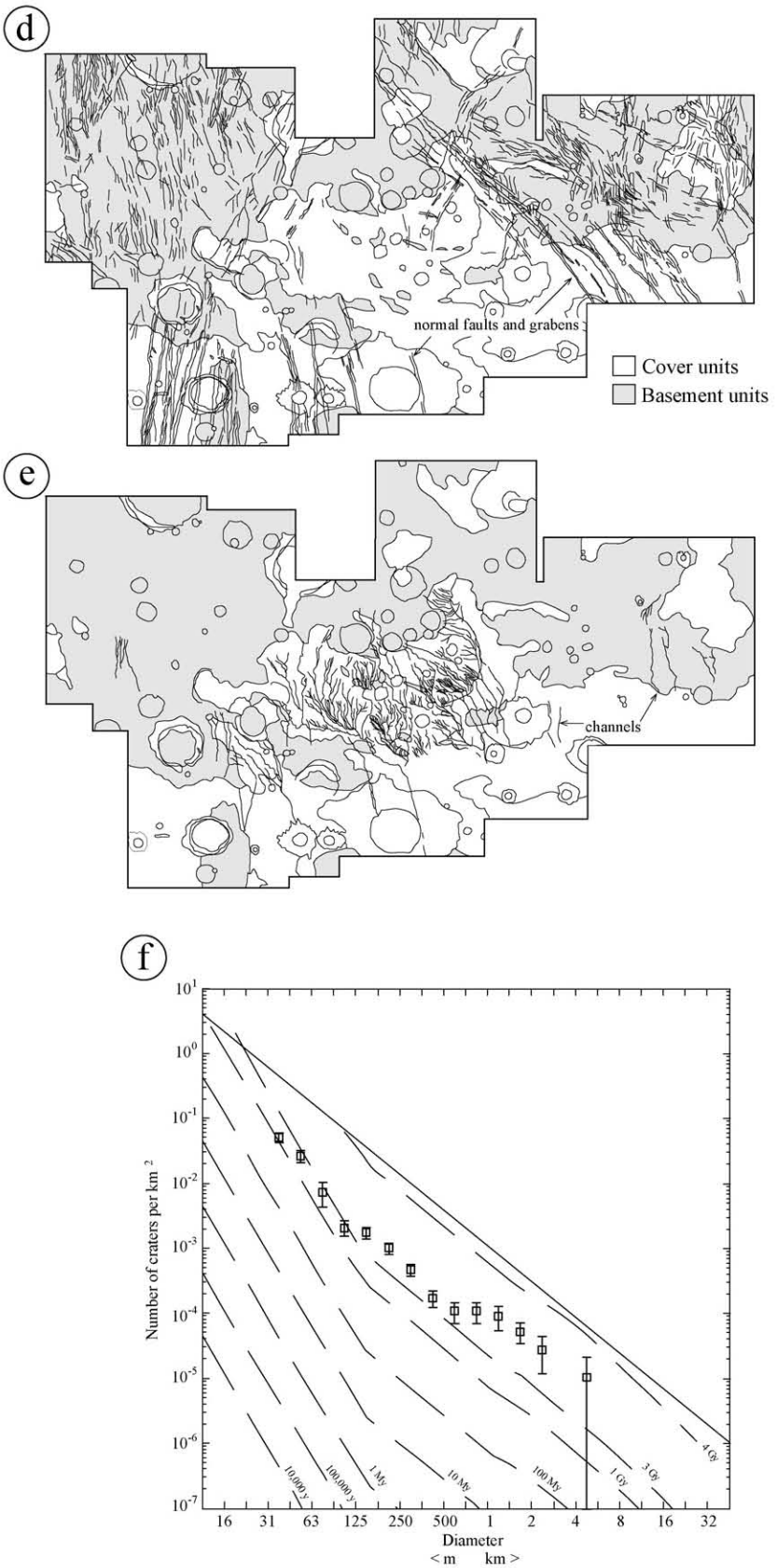

Fig. 5. (*continued*)

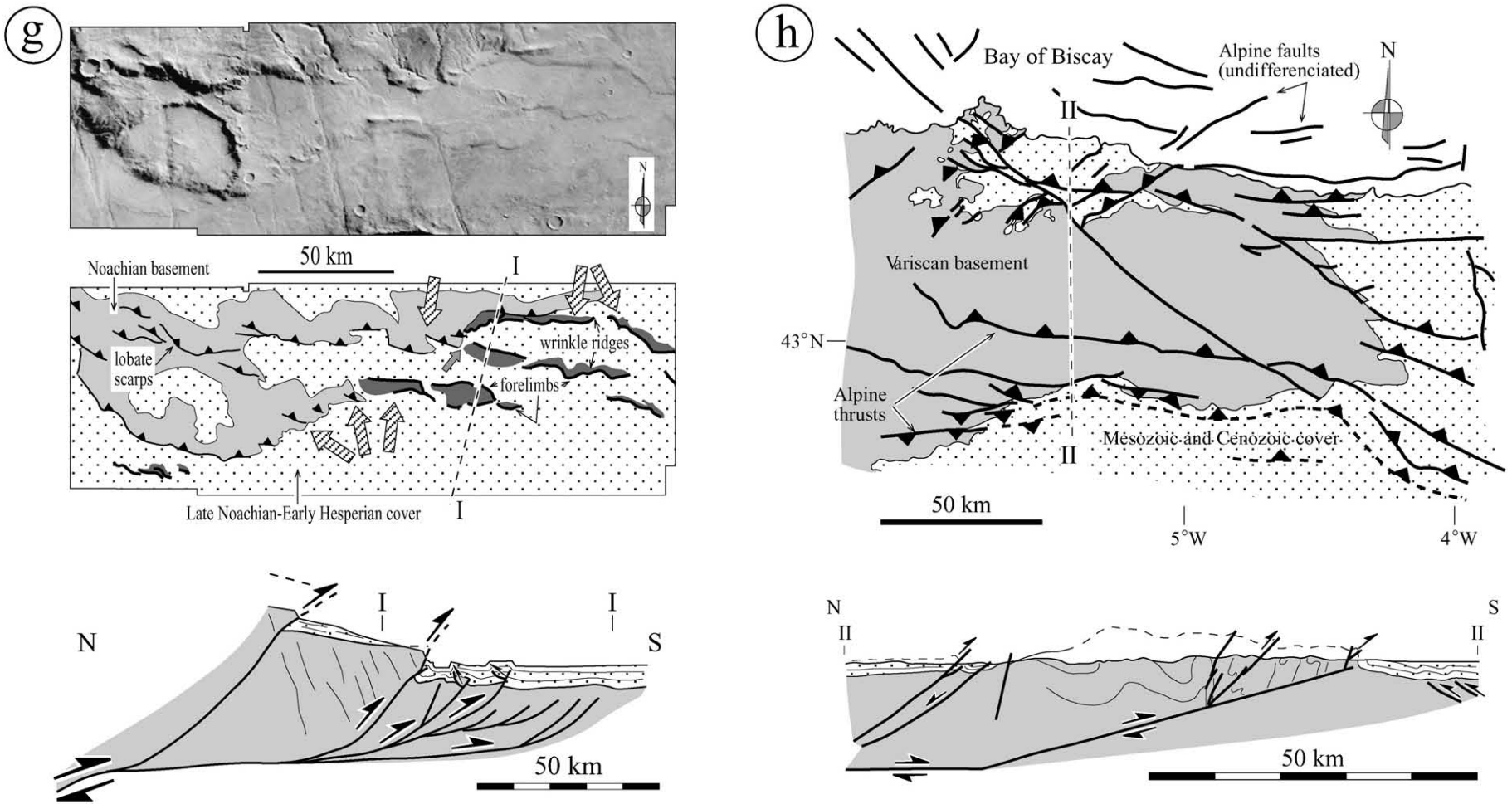

Fig. 5. (*continued*)

Valles is best interpreted as due to top-to-the-south movement along northward dipping thrusts. Lobate scarps show branching and en echelon geometries, a trait especially clear around 44° S 92° W (arrows with oblique pattern in Fig. 5g). The en echelon array of thrusts near the center of the studied area can be read as a result of the activity of a NE–SW-directed, sinistral transfer zone. In the eastern side of the transfer, thrusts appear displaced northwards, and they even change to blind structures, only noticeable as tilted patches of basement and cover. Another transfer zone can be detected at the easternmost mapped area, where the layering describes a convex-southward arch (black arrows in Fig. 5c).

Wrinkle ridges follow the same en echelon layout (arrows with an oblique pattern in Fig. 5g) as lobate scarps do. Ridges on Mars are interpreted as fault-related folds affecting a layered cover that rests on a stiff basement (Watters, 1991; Schultz, 2000). En echelon bands show 60°–70° E azimuths, while individual segments of lobate scarps and wrinkle ridges trend 90°–105° E. Warrego Valles ridges geometry should therefore reflect the en echelon, branching shape of basement thrusts. Lateral transition between lobate scarps and wrinkle ridges near the center of the studied area (Fig. 5g, gray arrow) is an outstanding example of the relationship of martian basement thrusts and cover wrinkle ridges, a connection supposed but not proved up to now. This figure features also an ideal cross section through the zone of transit between scarps and ridges. The structural style, in map and section, is very similar to the observed at some Earth fold belts, as is for instance the central-western Cantabrian chain, west of the Pyrenees, Spain (Fig. 5h). Since there is no decollement layer, Alpine thrusts of this belt systematically cut across the Mesozoic and Cenozoic cover, and reactivate the basement Variscan structures (Alonso and Pulgar, 2004), in the same manner that basement is mobilized at Warrego area.

Zone E is centered at 32.5° S 84.5° W (Fig. 6), in the central part of Thaumasia Highlands, near the southern boundary of Solis Planum. North–south trending folds affect the layering of the Noachian basement (essentially the Nf unit, Fig. 6a), which are crosscut by younger N–S and ~65° W trending grabens. The orientation and style of these folds are similar to those of Zone B, and they probably correspond to the second generation of folds observed in Zone C.

Zone F (Fig. 7) is centered at 25° S 58° W, in the highlands called Nectaris Fossae, the easternmost part of Thaumasia Highlands. The main structural element of this area is an outstanding regional unconformity between the Noachian basement and the Hesperian cover (see below), with different ages confirmed by the crater counts (Fig. 7a). The basement occupies a topographic high whose eastern border is a N–S-directed, slightly curved line (Figs. 7b and 7c). On both sides of this contact the layering dip changes abruptly, being always steeper on the cover layers than on the basement ones (unconformity marked in Fig. 7d). The direction of the basement layers intersects obliquely to the contact, therefore the cover cuts deeper basement units as one goes northwards, while the cover layering keeps parallel to the contact. Since the cover is horizontal away from the contact, it is clear that this block has been rotated. If this layer is rotated back unto the horizontal, the basement layering would be E–W-directed with a gentle dip to the south. An intriguing feature common to both units (and indicated by a white arrow in Fig. 7d) is a highly curved arch of the layers in the southern part of the contact.

Lobate scarps have not been identified within Nectaris Fossae. On the contrary, wrinkle ridges appear well developed (Fig. 7d). Most of the wrinkle ridges are N–S-directed, with forelimbs on the eastern slopes, though wrinkles with westerly-oriented forelimbs, or forelimbs on both sides, are also found (Fig. 7d). Two interesting features are observed on Nectaris wrinkles. The first one is the alignment of rhomb-shaped wrinkle ridges (Fig. 7e). These ridge chains are oriented NE–SW and NW–SE, i.e., oblique to the general alignment of wrinkle ridges. Their layout is identical to the one produced in the analog models of restraining stepover structures at strike-slip shear zones (e.g., McClay and Bonora, 2001, and our Fig. 7f). These push-up or rhomb-horsts structures are common on Earth (McClay and Bonora, 2001) where they commonly have sizes similar to the ones of their martian counterparts.

A second feature to highlight for the ridges is that their spacing progressively narrows (see Fig. 7d) as one goes eastwards, from around 60 km in the west to less than 20 km in the easternmost reaches of the unit. This spatial variation is an important element in the structural interpretation of this area. Applying the Montési and Zuber (2001) model, the depth of the detachment that originated these structures can be calculated. The result is a depth of 2.4 to 5.6 km under the eastern area of the cover and up to 7.7 to 15.3 km at the west, under the contact with the basement. We assume (following Schultz and Tanaka, 1994), that the structure is a buckling instability and not a localization instability (Montési and Zuber, 2001), since this last option would add an order of magnitude to the above figures. A detached cover hundreds of kilometers thick would go against the association of the wrinkle ridges to only the cover units (Fig. 7d). The thickness of the layered units measured in Valles Marineris walls (Robinson and Tanaka, 1988; McEwen et al., 1999), 600 km from this area, is also reasonably comparable to the Nectaris cover. It seems clear, in any case, that the depth to the basal detachment increases from east (<5.6 km) to west (>7.7 km): Therefore, the detachment dips to the west. The mean dip of this detachment can be estimated between 0.6° and 3.7°, an acceptable value from a mechanical point of view as it coincides with, among others, the estimated values for the Himalayan or Taiwan thrust wedges (e.g., Dahlen et al., 1984). This geometry is similar to the ones at external zones of Earth orogenic belts, where deformation affects only the upper crust, detached from its basement (thin-skinned tectonics). For this model to be mechanically feasible, a generalized detachment layer between basement and cover is needed. In the martian case, a hypothesized (and discussed; Mège, personal communication) megaregolith (Zuber and Aist, 1990; Schultz, 2000) or any weak unit at the cover base (Zuber, 1995) could be sufficient. As for the detachment limits, its extension towards the east seems logical: probably it tapers out in the area of closely spaced ridges, which limits with an exhumed basement zone to the east. The detachment prolongation towards

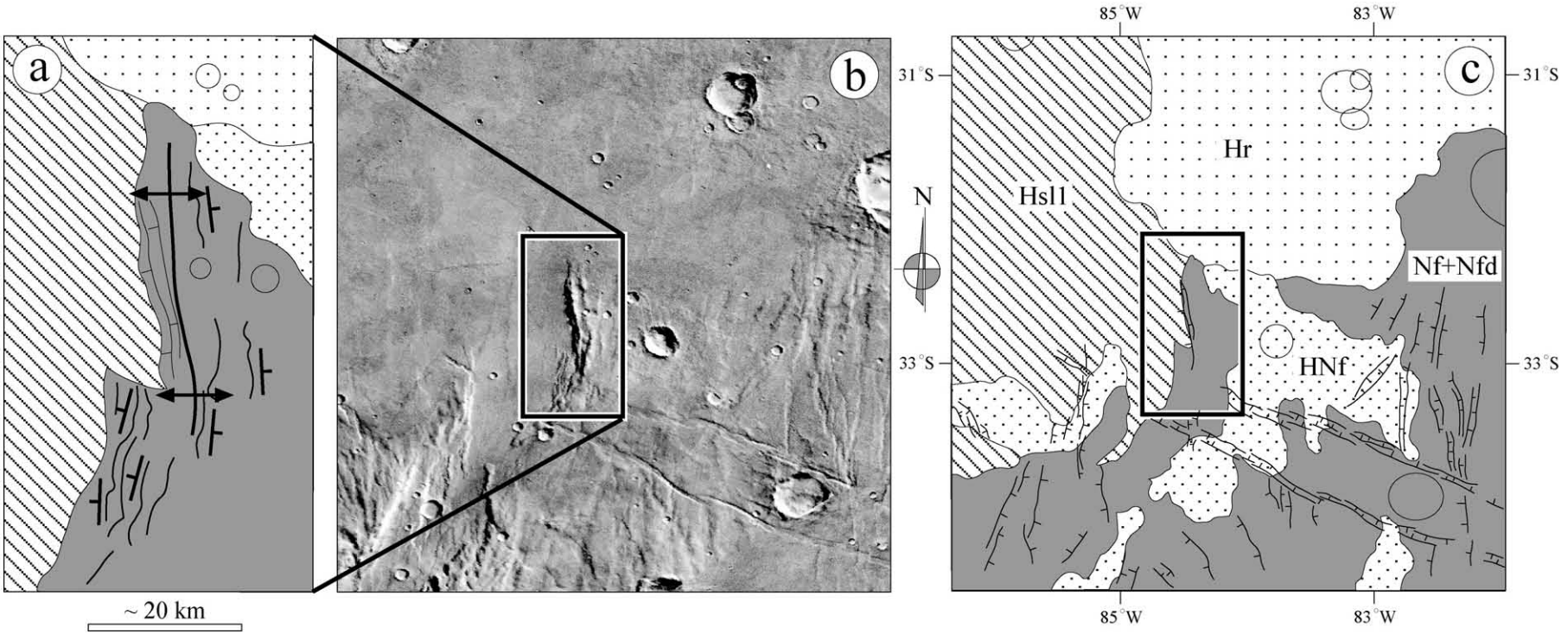

Fig. 6. Image and structural interpretation of Zone E. (a) Geological interpretation of the structure of the area marked in (b). Geologic units as in (c). (b) Context image. (c) Geological map of the area covered by the image, modified from Dohm et al. (2001). Nomenclature of geologic units according to Dohm and Tanaka (1999).

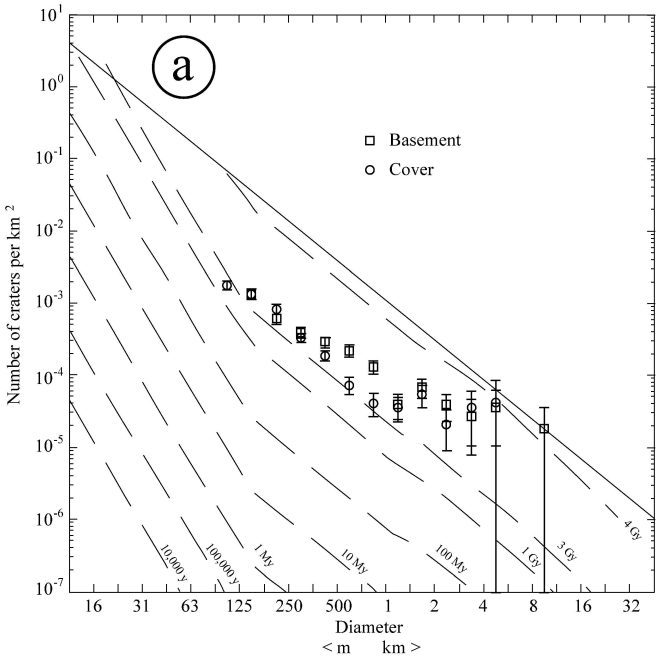

Fig. 7. Zone F, Nectaris Fossae. (a) Crater count curves. The older, thrusted basement (squares) shows more craters than the cover (circles) between 0.25 and 2 km, while both populations show saturation for diameters >5 km, what implies old resurfacing processes. (b) Reference mosaic of the studied area. (c) Geologic map (modified from Dohm et al., 2001). (d) Map of compressive structures. The white arrow marks a region with tightly curved layering, southward-looking convex. (e) Detail and structural interpretation of the areas outlined in (b). (f) Models and Earth examples of push-up structures similar to the ones portrayed in (e) (modified from McClay and Bonora, 2001). (g) Structural sketch of the cover east of Nectaris Fossae, with an insert of the typical layout of thrusts produced by indentation of a rigid block (modified from Crespo-Blanc and González, 2005), and an ideal cross section through the main thrust front. Black arrow marks the location of the basement-cover unconformity. (h) The Himalayas as a Nectaris Fossae fold and thrust belt analog. (i) Geologic sketch and schematic cross section through the Pyrenees basement and foreland (modified from Capote et al., 2002). (j) Extensional structures. (k) Drainage channels.

the west is more problematic, since the dip of the unconformity suggests that in this area (black arrow in Fig. 7g) the detachment involved the basement itself. The importance of the unconformity slope and of the basement topographic high could be a consequence of thrusting a big crustal block over a frontal ramp, the typical example of a thick-skinned tectonics. Vertical forces also can generate upward arching of the basement, but the high dip of the unconformity (Fig. 7g) needs unreasonably high vertical displacements. The geometrical relationship between the uplifted basement and the wrinkle ridges in the nearby cover (Figs. 7d and 7g), with no solution of continuity, is easier to explain in a bulk contractional setting.

It is important to highlight that both thin- and thick-skin tectonic styles are connected laterally at Nectaris in the same way as in terrestrial mountain belts. All described structures can easily be interpreted as the result of the tectonic thrust of the Thaumasia block towards the east over Aonia Terra. The similarity between Nectaris Fossae and terrestrial orogenic belts is reinforced when we consider the arched geometry of thrusts and folds. Analog models of orogenic belts produced by indentation of a rigid block (e.g., Crespo-Blanc and González, 2005; insert in Fig. 7g) show traits comparable to the ones described at Nectaris. Similar features have been described on the Himalayas, including recent extensional structures roughly normal to the thrusts (Fig. 7h). Even more suitable seems the analogy with the Pyrenean belt, where Eurasia and Iberia collided without intervening oceanic lithosphere (Fig. 7i). The cross section through Nectaris Fossae features a crustal architecture strictly comparable (excepting for its bigger size) to the one shown on the ECORS-Pyrenees section through the southern-central Pyrenees (Fig. 7i). On both the Himalayas and southern Pyrenees, pure or transpressive megashears are active at the side areas of the arched zones, and their geometry is identical to the push-up alignments at Nectaris. Even the thrust vergence can be compared with terrestrial analogs. On Earth, the vergence points towards the foreland in absence of a detachment layer. On the contrary, the vergence is variable when such a layer is present, as is the case for the southern Pyrenees or Nectaris. In contrast, Warrego Valles shows predominantly thick-skinned structures, with little evidence of thin-skinned tectonics. We thus compare Warrego Valles with the central-western Cantabrian Mountains, which is the western prolongation of the Pyrenees. Following this terrestrial analog, it can be suggested that the basement-cover surface lacked a detachment layer in Warrego Valles. Transition from thick-skinned to thin-skinned tectonics across the mountain belt, such as in Nectaris Fossae or the southern Pyrenees, needs the presence of a generalized detachment layer.

Normal faults and grabens (Fig. 7j) cut all previously described structures. Most of them are oriented in a general E–W direction, orthogonal to the layering and also to the contact, but an older, strongly eroded set, runs N–S. Drainage at Nectaris Fossae forms a slightly centrifugal network (Fig. 7k) from the highlands to the ridged plains. Channels follow maximum dip on the basement and the cover as well. As in Warrego Valles, the drainage is severely controlled by the structures.

Zone G (Fig. 8), centered at 41° S 122° W, is located to the south of Daedalia Planum. An old, probably Noachian (?) basement with a penetrative ~60° W trending layering alternates with a less cratered cover, probably Hesperian or Late Noachian–Early Hesperian. Lobate scarps in the basement and wrinkle ridges in the cover are the main compressive structures in the area (Figs. 8a and 8b). Similarly to Warrego Valles, lobate scarps limit ~60° W-directed bands of uplifted basement and are sub-parallel to the basement layering. Wrinkle ridges in the cover are similar to those of Nectaris Fossae, with the presence of rhombic geometries attesting for the activity of wrench or transpressive shear zones in the basement. Scott and Tanaka (1981) mapped several volcanic constructs cropping out through the basement (Fig. 8b) and dissected by radial drainage patterns (Fig. 8c). The alignment of these volcanic centers along ~60° W trends, and their spatial association with lobate scarps suggest a tectonic control of the volcanic activity. The structural interpretation of these compressive structures (Fig. 8d) explains the ~60° W alternating basement-cover bands as pop-up and pop-down structures. These structures are limited by basement thrusts that caused the lobate scarps and wrinkle ridges. The vergence of these thrusts is essentially towards 150° W, but

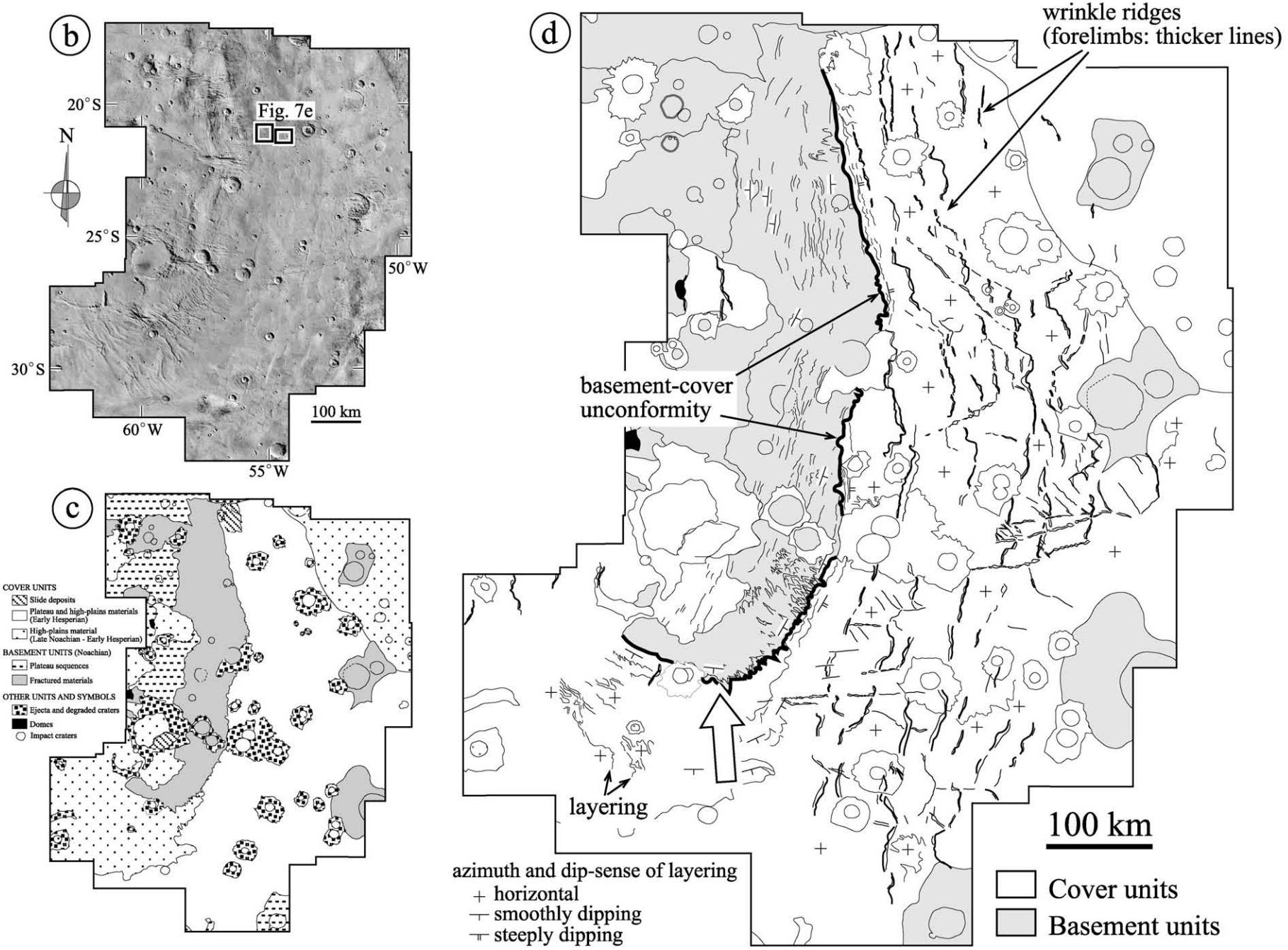

Fig. 7. (*continued*)

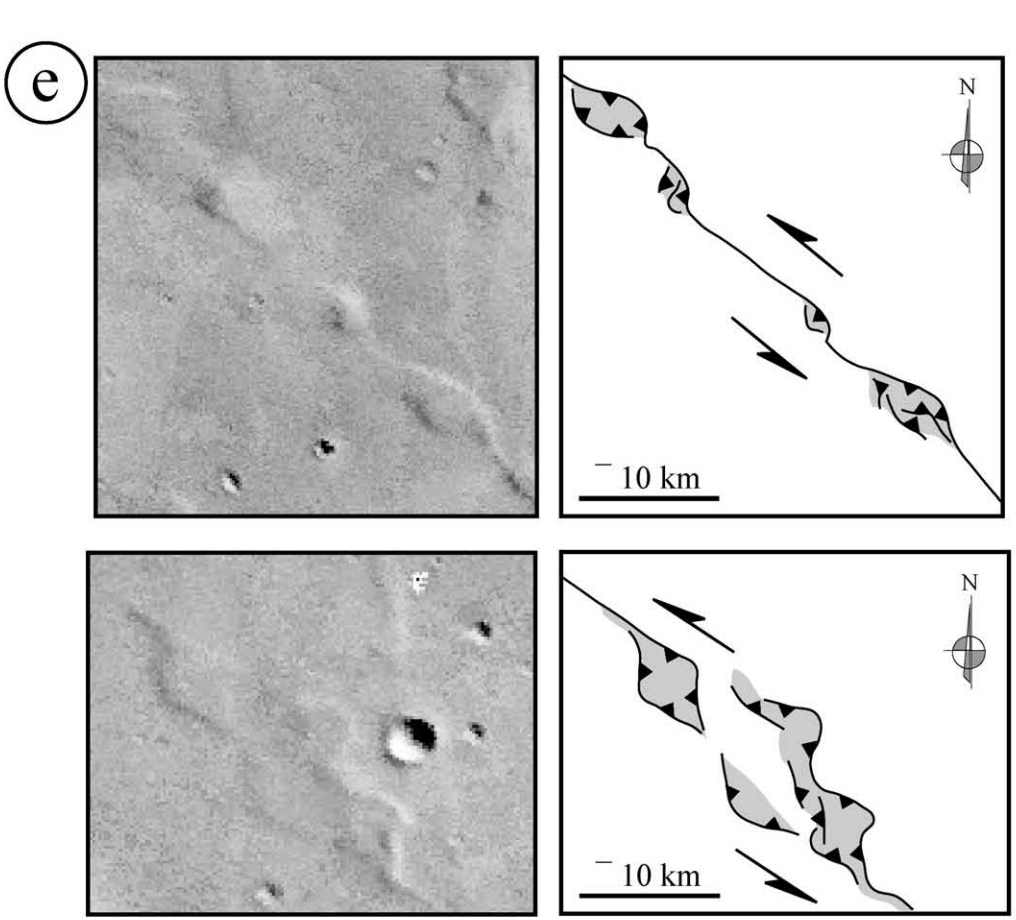

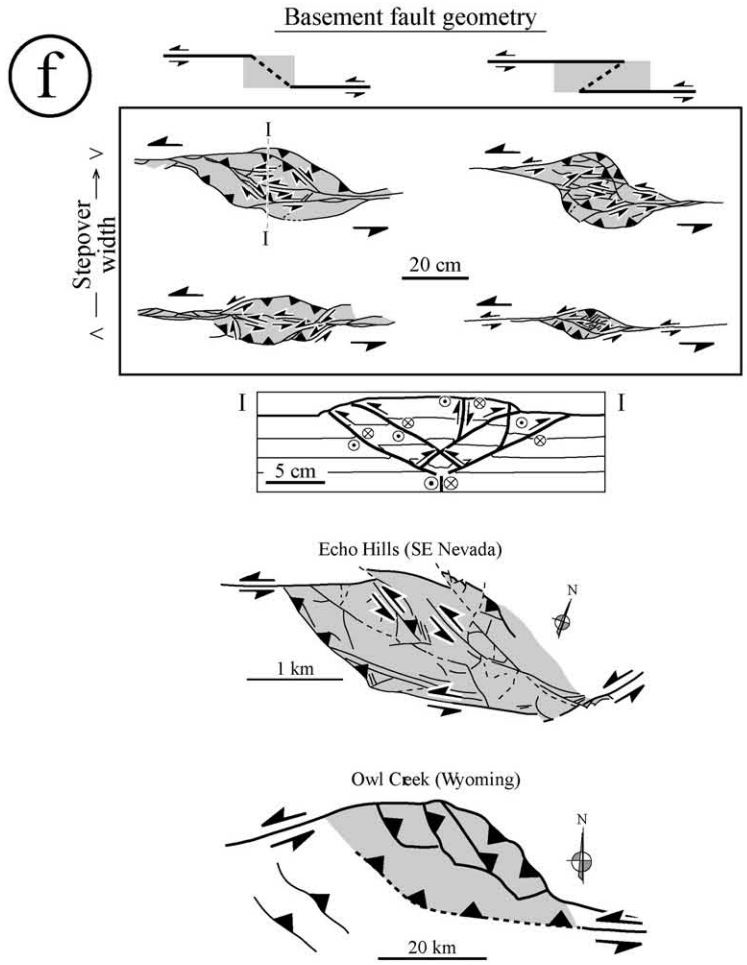

Fig. 7. (*continued*)

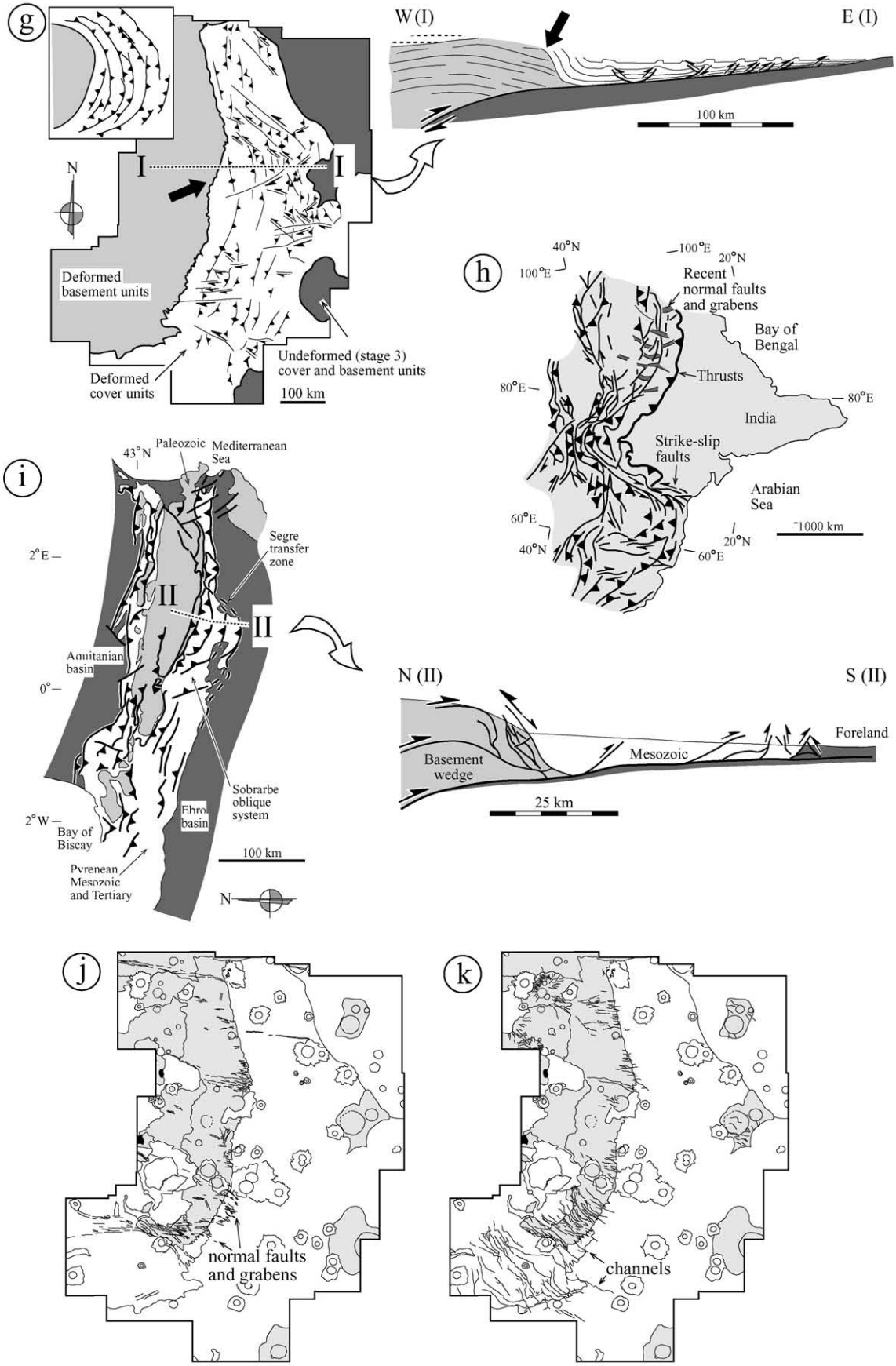

Fig. 7. (*continued*)

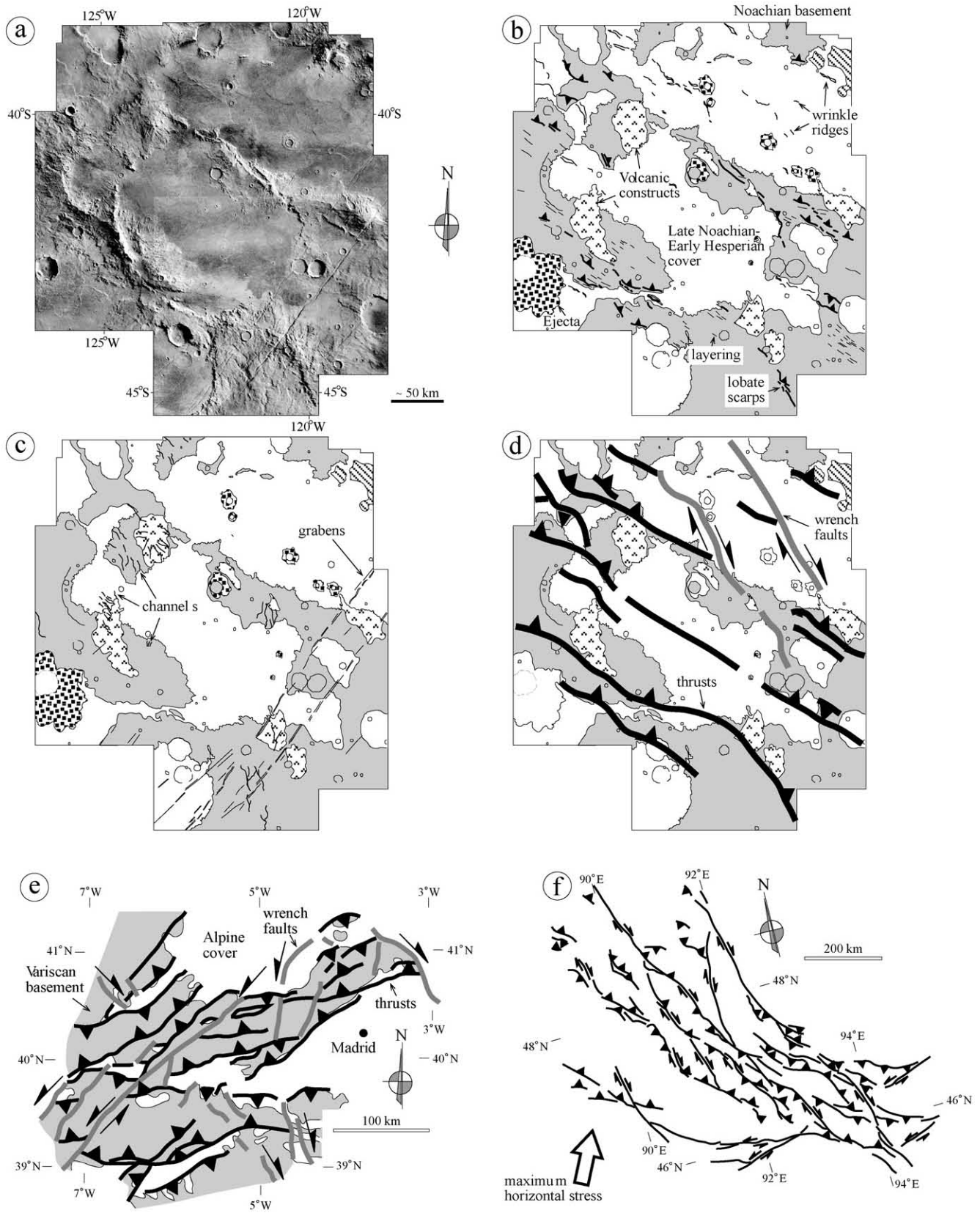

Fig. 8. Zone G (see Fig. 1) in the Icaria Fossae area, south of Daedalia Planum. (a) Reference mosaic of the studied area. (b) Geological map with location of the main compressive structures. (c) Drainage pattern and graben structures. (d) Simplified structural sketch with interpretation of the relative displacements along wrench faults and thrusts. (e) Sketch of the main Alpine structures at the central part of the Iberian Peninsula (modified from Álvarez et al., 2004). (f) Map of late Cenozoic faults in the Mongolian Altai, modified from Cunningham (2005). The obliquity between the far-field deviatoric stress with horizontal maximum compression axis (large white arrow) and the main faults of the area originates a regional-scale dextral transpressional duplex.

some ~30° E-vergent thrusts are also evident. These thrusts are locally displaced by coeval wrench faults that probably acted as transfer structures.

The structural characteristics of Zone G are comparable with those of the Alpine structures at the central part of the Iberian Peninsula (Fig. 8e). Note, in particular, the presence in both zones of uplifted basement blocks limited by thrusts, and separated by pop-down structures filled by cover units. Sectors with distinct thrust-fault architecture in plan-view are limited by large wrench faults. The mountain ranges in this zone of Iberia are explained as the response of the Iberian foreland to deformation along the Betic orogen, a belt located at the boundary between the Iberian and African plates (Álvarez et al., 2004). Comparison of Zone G with the Mongolian Altai is even closer (Fig. 8f), as revealed by the map-view pattern of faults, and even by the trends of thrusts and strike-slip faults (compare Figs. 8d and 8f). The Mongolian Altai is a far-field deformation response to the Indo-Eurasia collision (e.g., Cunningham, 2005). As for scale, the Altai, located 2500 km to the north of the Himalayan belt, is 250 km wide and therefore similar to Zone G, which is 600 km to the southwest of the Thaumasia Highlands and is around 200 km wide (Fig. 8b). More important than scale is that Zone G, just like the Mongolian Altai, does not show the thrust-wedge architecture typical of orogenic belts and displayed in the Thaumasia Highlands boundary (Warrego Valles or Nectaris Fossae). Rather, the structural style is dominated by 60° W-striking thrusts and ~30° W-striking dextral strike-slip faults (Fig. 8d). In addition, restraining bends and thrust ridges are common both in Zone G and in the Mongolian Altai, and the Asian belt shows a strong correlation between the strike of Cenozoic faults and the orientation of the previous Paleozoic foliations. The same structural control is also observed in Zone G, where lobate scarps and wrinkle ridges are parallel to the Noachian layering (Fig. 8b). By terrestrial standards, Zone G represents a far-field mountain belt associated with the ~30° E-directed collision of the Thaumasia block with Aonia Terra–Daedalia Planum, acting as a foreland thrust followed by later 30°–35° E-trending normal faults and grabens crosscutting the described compressive structures (Fig. 8c).

Zone H (Fig. 9a), centered at 45° S 67° W, is located at the center of Aonia Terra. The structural characteristics of this zone are very similar to those of Zone G and corresponds to a region of Noachian basement dominated by lobate scarps, and small basins of Late Noachian–Early Hesperian cover, probably with a thin infill of sedimentary and volcanic rocks. The alignment of lobate scarps at the center of the image marks the NW limit of the central basin. Following the interpretation of Zone G, Zone H can also be considered as a far-field mountain belt resulting from the collision at the border between the Thaumasia block and its foreland thrust (Aonia Terra). At present, the thrusts (lobate scarps) trend in a 30°–35° E direction. This is in contrast to the basement layering, which reflects the large-scale structure of the Noachian crust and strikes ~70° W. The misaligned orientation of the far-field deformation axes with respect to the Noachian structural grain might explain why Zone H displays a narrow (50–100 km) deformation belt in comparison with Zone G (200 km); its simpler deformation pattern contains only one main thrust (Fig. 9b).

Zone I (Fig. 10a) covers an area centered at 39° S 48° W at Nereidum Montes, the rugged semicircular terrain north of Argyre Planitia. Tanaka et al. (1998) noted that this chain bore traces of tectonic deformation, an observation confirmed by our structural interpretation (Fig. 10b). Layering appears strongly tilted (see the cuesta and hogback morphologies in Fig. 10a), forming large (~200 km), NW–SE-directed antiforms and synforms whose axial traces show a sinuous geometry. This can be explained by the presence of an additional NE–SW fold set which interferes with the NW–SE-trending folds. Overall, this region features a complex pattern of superposed folding processes, with the NW–SE structures forming first, and followed by the appearance of the NE–SW folds. The coincidence in shape and size of these structures with Zone C folds needs to be stressed, since it reinforces the idea of a structural community between Thaumasia Highlands and extra-Tharsis places like Nereidum Montes, two points some 2500 km apart. Another key observation is that the NE–SW folds axial traces are roughly parallel to the Nectaris Fossae thrust front. They are therefore compatible with the same stress tensor that created the Thaumasia Highlands structures. As for the NW–SE folds, they must belong to a former tectonic phase. The crater count statistics (Fig. 10c) is more limited than the one at Zone C, but the portrayed bins are very similar in the 0.2 to 1.5 km range. This coincident age could probably mean that both areas represent the exhumed roots of the same geologic unit.

4. A tectonic interpretation: the Thaumasia–Aonia Orogen

In what follows, we will try to show that the preceding data are sufficient to prove that an orogenic chain at least 5000 km long and 2000 km wide was built through stress fields with horizontal maximum and intermediate compressive stress axes, starting not earlier than 4 Gyr and ending not later than 3 Gyr. To start with, a long period of contractional deformation is required to form giant fold interference structures as the ones extant at Zones C (Claritas Fossae) and I (Nereidum Montes). On Earth, these fold interference patterns are typical features of the crystalline core-zones of orogenic belts. The sizes of these structures are also indicative of thick crustal units. Therefore, it is suggested that a 2000 km-wide belt comprising the Thaumasia Highlands and the outer surrounding area is the core-zone of a long-lived, essentially Noachian–Hesperian orogenic belt. More detailed images and rock sampling are necessary to check the possible exposure at these areas of rocks with structures indicative of ductile deformation. On the contrary, the structural characteristics of the rest of the studied zones, and those of the later stages of folding and thrusting in Zones C and I, seem comparable to those of the orogenic foreland (external) fold-and-thrust belts on Earth. This observation supports the hypothesis of Dohm and Tanaka (1999), who postulated the southeastern part of the Coprates Rise as an orogen comparable with the Wind River Mountain Range. Interestingly, these giant folds do not affect the Hf unit, a fact suggesting that the orogenic activity waned before Late Hesperian.

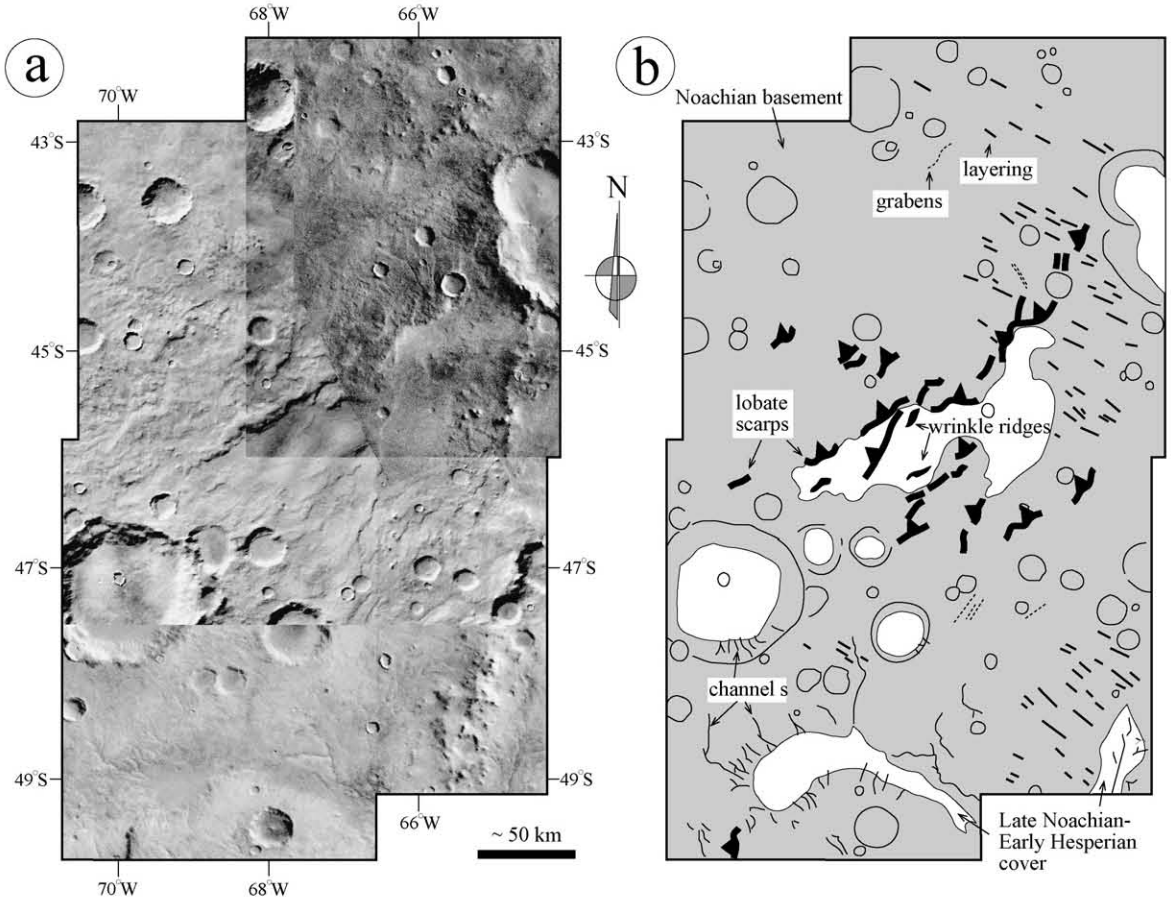

Fig. 9. Image and structural interpretation of Zone H. (a) Reference mosaic of the studied area. (b) Geological map with location of the main compressive structures affecting the zone. Drainage patterns and graben structures are also shown.

Since the core-zone folds are not concentric to the Thaumasia Plateau, they were formed prior to the inception of the present Tharsis volcano-tectonic bulge. If this is the case, they should not be associated with the regional uplift. As an alternative, we propose that the Thaumasia Highlands (and specifically the basement complex [Nb] and the older fractured material [Nf] of Dohm and Tanaka, 1999) represent the exhumed and eroded remnants of an old orogenic belt, for which, and basing on its extension towards the outer terrains (and especially to Aonia Terra), we therefore propose the name of Thaumasia–Aonia Orogen. This belt bears the record of at least four tectonic stages:

- Stage 1: Represented by the large folded structures (Figs. 4 and 10) of the basement ("Hill Unit" of Dohm and Tanaka, 1999). The original geometry of these structures at this stage is difficult to reconstruct because we have only isolated pieces of an ancient belt, tectonically disrupted by subsequent orogenic phases. The identifiable remaining structures are essentially E–W-directed in Thaumasia and they strike NW–SE in Aonia Terra.
- Stage 2: Tectonic activity produced long, tight folds (Figs. 3, 4, 6) generally oriented N–S (NW–SE at Zone C). Their coherent geometry contrasts with the disjointed orientation of the large folds, and their short wavelength requires the presence of a thin, folded layer. All these observations imply a long quiescent period between Stages 1 and 2, during which the basement materials, along with their big folded structures would have been deeply eroded. In fact, it is this exhumation by erosion which permits us to see the roots of the orogen (Phillips et al., 2001).
- Stage 3: During Stage 3, the Thaumasia Plateau moved towards the west, south and east producing the thrusts that can be identified on its border (Figs. 2, 5, 7), plus the ones at Aonia Terra and Daedalia Planum (Figs. 8 and 9). Some of these structures could represent escape structures, as first proposed by Webb and Head (2002). These thrusts cut the folds of Stages 1 and 2, and cover the Icaria Planum impact basin.
- Stage 4: During this closing stage, grabens cutting across all the previous structures were produced, probably as a consequence of post-orogenic gravitational spreading. The most important were those of Claritas Fossae, radial to the Syria Planum volcanic center.

The Thaumasia–Aonia Orogen appeared sometime between the Noachian and Early Hesperian times. The best time reference is the deformation of Nereidum Montes, which attest that

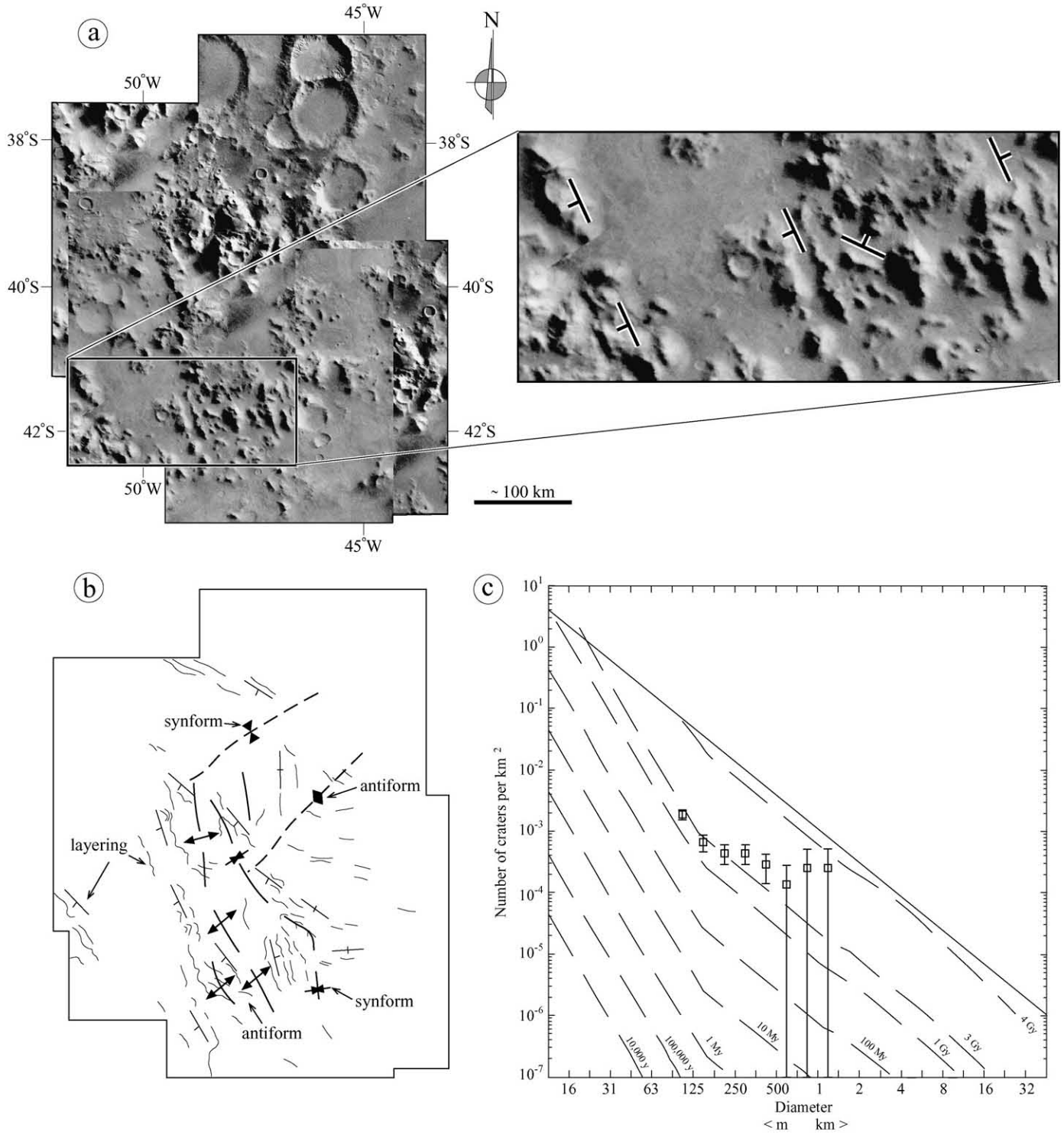

Fig. 10. Reference mosaic (a) and structural interpretation (b) of Zone I, at Nereidum Montes (see Fig. 1 for location). Close-up view of a selected zone of the reference mosaic is shown to appreciate the cuesta and hogback morphologies that allow reconstructing the large-scale folding structure of Zone I. Continuous and dashed lines mark the first and second generation of folds, respectively. (c) Crater count statistics (see text for interpretation).

Stage 1 postdated the Argyre impact. If we assume the typical age attributed to the major impact basins of 4 Gyr, we conclude that the orogen first appeared in the Middle Noachian. The presence of an erosional period after Stage 1 requires a quiescence period in Late Noachian or Early Hesperian. This is in agreement with Solomon et al. (2005), which proposed widespread and intense tectonic movements in Mars' western hemisphere during the Middle Noachian or Early Hesperian.

The explanation of tectonic structures forming 4 Gyr ago, and now cropping out as isolated patches, is no easy matter.

Deformation of a thick crustal layer is in any case needed to explain the appearance of folds 200 km long. This, and the bulk of our structural analysis lead us to propose that a period of lithospheric mobility was the responsible for Stage 1 structural features. The many shortcomings (Pruis and Tanaka, 1995) of the plate tectonics model advanced by Sleep (1994) are not applicable to our orogenic hypothesis, since the original paleotectonic maps of this author (Sleep, 1994) were limited to the northern lowlands, far from the Thaumasia Highlands and Aonia Terra. The most recent gravity data (Zuber et al., 2000) place the dichotomy at the western border of the Thaumasia Plateau, and therefore qualify this area as a suitable place for subduction and collision tectonics. The reconstruction of the geometry of the chain is nevertheless beyond our present knowledge of martian Noachian geology. The best we can say by now is that the Stage 1 structures seem to require a powerful, long cause of lithospheric deformation comparable to those produced on Earth at convergent plate margins.

Identifying regional compressive stresses in Stage 2 presents a slightly easier case than for Stage 1, since most folds have a coherent roughly N–S orientation. A regional E–W-directed compressive stress field would suffice to explain the observed data, but it is clear that the lithosphere as a whole was not affected during this period: instead, a thin-skin tectonics deformation of the upper crust is observed. In view of the pervasive deformation and direction of the stresses, we propose that this stage formed during a residual phase of plate tectonics, in the line advanced by Fairén and Dohm (2004).

At Stage 3, it appears that Thaumasia Plateau behaved as a rigid block for the first time, an indenter which thrusted the terrains to the west, south and east. As a result of this thrusting, Thaumasia Highlands mountain belt was formed, and its ~70 km-thick crust is a token of the violence of the thrust (Zuber et al., 2000). Different gravitational processes have been envisioned for this tectonic stage. Dohm and Tanaka (1999) proposed that deep crustal intrusions made a buoyant crust whose uplift created the fold-and-thrust margins; Webb and Head (2001, 2002) put forward a gravitational giant southeastwards-directed movement from the huge volcanic construct at Syria Planum. The plume (or superplume) widely postulated (Mège and Masson, 1996b; Maruyama et al., 2001; Dohm et al., 2001) under the Tharsis bulge has been considered to provide sufficient lateral momentum for the thrust. With the enormous thrust, the plateau rim crust thickened, lifted up and its already eroded basement was rejuvenated. During this period, erosion was probably very active due to the climatic effects of the volcanism (Head et al., 2001). The snake-like folds observed in Zone C are indicative of the intensity of the erosion processes before the generation of the Stage 3 folds.

Finally, all Stages 1, 2 and 3 structures were cut by normal faults and grabens under an extensional tectonic regime: the Claritas, Thaumasia and Icaria Fossae systems were formed at this closing stage (Dohm and Tanaka, 1999). Some large exposures of the basement complex appear at the uplifted footwall of these extensional systems (as, for instance, in the western part of Fig. 4a). The youthful character of these structural sets suggests a transition from contractional to extensional tectonics in the Thaumasia Highlands. However, the presence of some old and strongly dissected E–W grabens could be indicative of extension coeval to the folding episodes, representing either intervening extensional stages or local accommodation structures.

5. Discussion

While any martian plate tectonics theory (Sleep, 1994) has still many questions to answer (Pruis and Tanaka, 1995), this idea is clearly permeating an increasing number of papers on Mars and even on other planets [see Romeo et al. (2005) for a Venusian case]. Recent martian examples include Frey (2003, 2004), Spagnuolo and Dohm (2004), Connerney et al. (2005) and Christensen et al. (2005). One of the strongest points of this theory is that it provides an easy explanation for the primordial Mars magnetic field (e.g., Nimmo and Stevenson, 2000). In this respect, however, our orogenic calendar is rather unsatisfactory, for we are proposing that plate tectonics began to give shape to the Thaumasia–Aonia Orogen starting at 4 Gyr, just the time when the magnetic field was apparently on the wane.

This problem is not new, though, in martian geology. Only recently the magnetic stripes identified on the northern lowlands (Connerney et al., 2005) have permitted us to interpret the dichotomy as a feature likely to have been formed through plate interactions (Smith et al., 1999; Watters and Robinson, 1999). But the time of cessation of the supposed recycling lithosphere regime is also a matter of contention. The lack of magnetic anomalies on the major impact basins has been considered to provide a date (~4 Gyr) for the end of lithospheric recycling, but these areas could as well have been demagnetized by the shock events (Hood et al., 2003). In any case, since the basins were not remagnetized, the core dynamo would have to be defused when the basins cooled (Solomon et al., 2005). Other researchers have proposed different solutions to this problem. Johnson and Phillips (2005) consider the possibility of magnetic field and a plate tectonics regime until Early Hesperian, with magnetization erased at Hellas and the lowlands. Fairén et al. (2002), Baker et al. (2002), and Fairén and Dohm (2004) maintain that plate tectonics declined very gradually, and that the core stopped convecting while plate movement was still active. This suggestion is concordant with our ideas on the Thaumasia–Aonia Orogen, which exhibits progressive lesser amounts of deformation. Other authors propose different durations for lithospheric recycling without confronting the magnetic field question. Hauberg and Kronberg (2001), for instance, allow plate movement until Early Hesperian. The most recent data on this debate, the purported identification by Connerney et al. (2005) of supposed transform faults almost 3000 km long seems highly speculative to the present authors, since their stronger argument, the offset of magnetic lineations (their Fig. 2) is based on a very small number of bands, whose reconstruction is by no means univocal.

Another point for discussion is the origin of the Thaumasia thrusts (our Stage 3). In our view, the gravitational hypotheses (Mège and Masson, 1996a; Dohm and Tanaka, 1999; Banerdt and Golombek, 2000; Webb and Head, 2001, 2002) face a kinematic problem, highlighted by the arrangement of

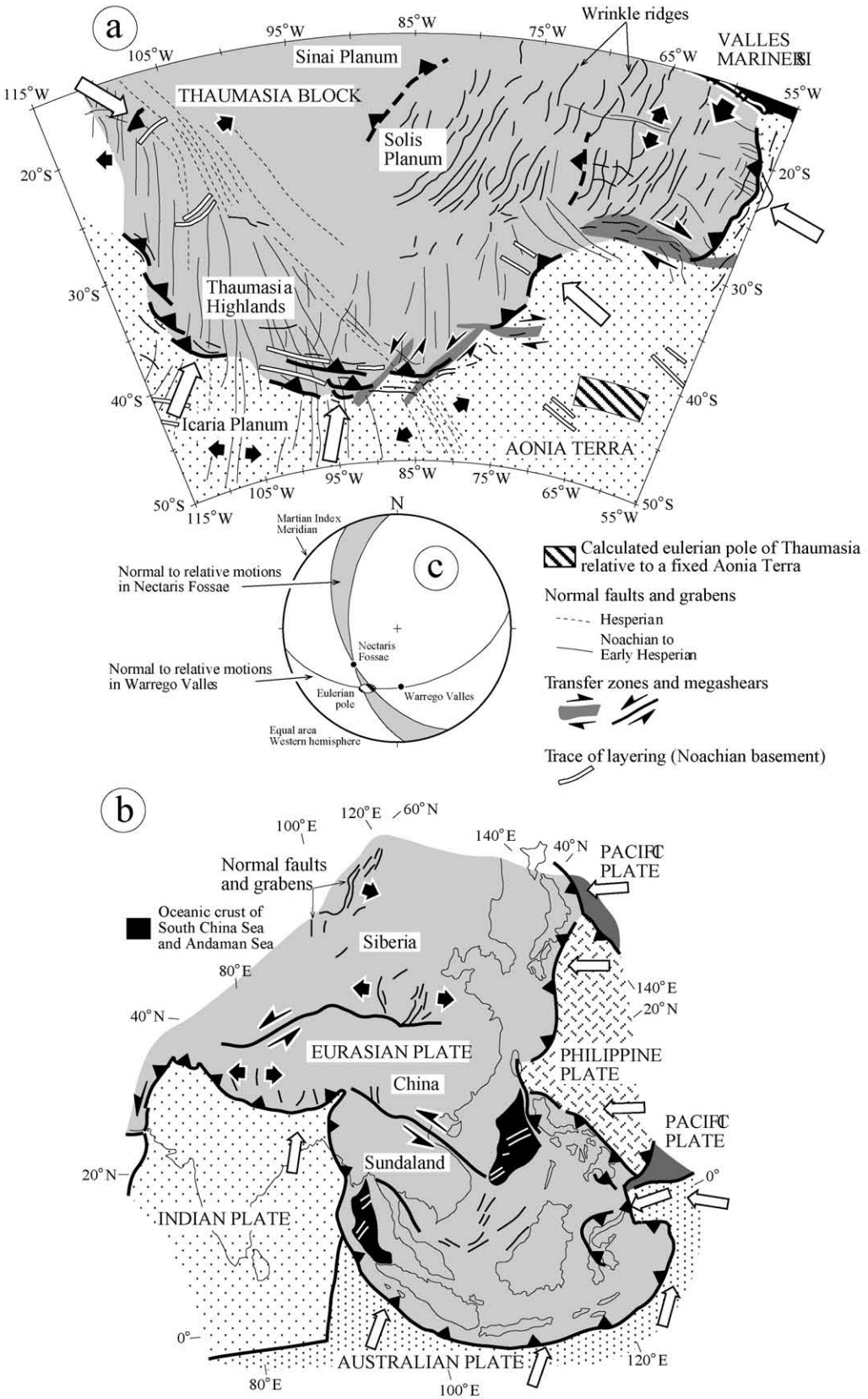

Fig. 11. The Thaumasia block (a) compared with the southeastern sector of the Eurasian Plate (b). Layering in the Noachian basement at Nectaris Fossae (around 25° S 58° W) has been tilted to its pre-Stage 3 position. Large white arrows indicate relative displacements at the studied sites of the Thaumasia boundary (a) and relative plate motions at distinct points of the Eurasian Plate boundary (b). Small black arrows indicate extension direction associated with normal faults and grabens. See text for discussion.

the relative displacement vectors in the margins of Thaumasia (Fig. 11a). The Syria Planum plateau is located laterally to Thaumasia, a situation incompatible with the displacement pattern observed along the Thaumasia borders. These vectors converge towards a zone located in the center of Thaumasia, somewhere between Sinai and Solis Plana. The fact that this is a zone with past and modern subdued topography (Anderson et al., 2004) renders improbable the hypothesis of gravity spreading in Thaumasia. Related to this problem is the possible comparison of the Thaumasia block with some of the Earth's lithospheric plates. Not only the dimensions, but also the structural evolution of this unit are very similar to the southeastern sector of the Eurasian Plate (Fig. 11), as can be summed up in the following points:

* Thrusting borders of orogenic type on all the front side.
* Different vectors of relative movement between the moving unit and its autochton (white arrows in Figs. 11a and 11b).
* Extensional zones roughly perpendicular to the shortening ones (black arrows at Figs. 11a and 11b). In any case, extension in Thaumasia is much lower than in any orogenic belt on Earth.
* This structural border explains the differential movement of the Thaumasia block: the northern part, comprising Solis and Sinai Plana and Nectaris Fossae, thrusted eastwards, while the southern province (Thaumasia Highlands) thrusted southwards. The earthly parallel stands: while Sundaland moves to the south, China overthrusts the Pacific and Philippine plates to the east. Valles Marineris could represent another escape structure, as advanced by Webb and Head (2001, 2002).

An evidence for the two Thaumasia subunits can be deduced from the impossibility to obtain a common Eulerian pole (Fig. 11c) for both. A possible solution for this problem is that the rest of the martian lithosphere were, like that of Earth, a mosaic of plates. An alternative is that the movements of the two subunits were not contemporaneous. This last explanation is supported by the martian chronology: the ridged cover is older at Warrego (Noachian–Hesperian) than at Nectaris (Early Hesperian). This can be read as an indication of deviatoric stresses with N–S horizontal maximum compression that triggered the shortening of Thaumasia in the same direction and the consequent southwards-directed thrusting movement of its southern border. Afterwards, the Thaumasia block should be unable to accommodate further shortening, so it was forced to extrude laterally, much in the same way as southeastern Asia after the Indian collision. Individualization and eastward escape of the Sinai–Solis–Nectaris block should have taken place at this moment. Westwards escape was probably hindered by the standing mass of Tharsis, which is comparable with the lateral escape of southeastern Asia favored by a free boundary on the east, and impeded by the large continental block of the Eurasian plate to the west. It is at this precise moment that the elevated topography of Syria Planum could have had a decisive influence on the tectonic evolution of Thaumasia. One set of graben would follow each movement, a fact that could explain the anticlockwise time variation of the extension direction in Warrego Valles (from N–S to ~25° W), and the presence of old N–S grabens at Nectaris Fossae.

Further support for our orogenic analog can be found in the linear gravity anomalies under the Thaumasia Highlands (Zuber et al., 2000). Orogenic belts on Earth typically show linear parallel belts of strong negative and positive free-air gravity anomalies (e.g., Bowin et al., 1981), very similar to those observed at the borders of the Thaumasia Plateau. Therefore, gravity and structural data coincide to support an orogenic tectonic setting for the Thaumasia Highlands. As for the negative belt, traditionally considered to be a signature of Tharsis load (e.g., Mueller and Golombek, 2004), it could be the martian equivalent of a foreland depression. Interestingly enough, the preliminary Bouguer map of Mars presented by Neumann et al. (2004) shows a prominent ring of negative anomalies along the Thaumasia highlands, a distinctive feature of collision belts on Earth due to the presence of mountain roots in a thickened crust (e.g., Park, 1988).

A more debatable set of data is the layering in the Noachian basement, which keeps an almost constant E–W to NW–SE trend along and across the studied area (Fig. 11a). We interpret this continuity as a strong indication of the huge size of this Noachian orogen (our Stage 1), amply exceeding the limits of the Thaumasia Plateau that would (as well as Tharsis) be a younger unit (our Stage 3). This represents an alternative to the "all Tharsis" classical hypothesis, which restricted almost any martian tectonics to the influence of the bulge.

The progress in reconstructing martian Noachian history is revealing features which in principle would need to be explained with global tectonic regimes, like the event that formed the lowlands and renewed the highlands as proposed by DeSoto and Frey (2005). Our contribution to this investigation is best portrayed in our Figs. 5, 7 and 11, where features of an ancient (>3 Gyr) Mars orogen are neatly comparable to structures in recent Earth orogens. Given the primitive state of our investigations on the primordial Mars, we still cannot tell whether this could be the sign of a profound unity among planetary systems.

Acknowledgments

We thank the Viking, Mars Global Surveyor, and Mars Odyssey teams for the use of Viking, MOC and Themis images. G. Cordero worked in this paper during a postdoc stage at the Universidad Complutense, Madrid, financed by Project IN104003 of DGAPA. J. García contribution was made possible by an ESA graduate stage during the summer of 2005, when Drs. Agustín Chicarro and Angelo P. Rossi provided a really helpful support. The manuscript benefited greatly from critical and thoughtful reviews by Robert C. Anderson and Daniel Mège.

Appendix A. Count crater data

Zone C

Image	Scale (m/pixel)	Latitude	Longitude	Surface (pixels)	$n > 125$ m (per 10^3 km)	$n > 1$ km (per 10^3 km)	$n > 2.83$ km (per 10^3 km)	$n > 8$ km (per 10^3 km)
e1701408[a]	5.91	−29.47°	102.65° W	507 × 8145	53	0	0	0
e1701825[a]	5.91	−28.38°	103.22° W	507 × 4008	25	0	0	0
e1801369[a]	5.90	−28.67°	100.32° W	509 × 5274	25	0	0	0
F460A11[b]	64	−28.16°	103.74° W	1204 × 1056	25	15	1	0
F460A13[b]	65	−28.79°	102.89° W	1204 × 1056	25	10	6	3
F460A14[b]	65	−27.83°	102.65° W	1204 × 1056	9	6	4	2
F460A15[b]	65	−29.40°	102.10° W	1204 × 1056	40	25	6	1
F460A16[b]	65	−28.42°	101.87° W	1204 × 1056	41	22	5	2
F460A17[b]	66	−30.00°	101.24° W	1204 × 1056	5	4	2	0
MI25S097[c]	231	−25.00°	97.00° W	1184 × 1280	6	6	5	1
MI25S102[c]	231	−25.00°	102.00° W	1184 × 1280	1	1	1	0
MI30S097[c]	231	−30.00°	97.00° W	1184 × 1280	47	47	38	16
MI30S102[c]	231	−30.00°	102.00° W	1184 × 1280	45	45	38	21
V07981003[a]	231	−29.00°	256.88° E	1407 × 3257	134	4	1	0
V09279002[a]	231	−27.23°	258.86° E	1405 × 3258	95	2	0	0

[a] MOC image.
[b] Viking image.
[c] Viking mosaic.

Zone D

Image	Scale (m/pixel)	Latitude	Longitude	Surface (pixels)	$n > 125$ m (per 10^3 km)	$n > 1$ km (per 10^3 km)	$n > 2.83$ km (per 10^3 km)	$n > 8$ km (per 10^3 km)
I05515005[a]	95	−38.28°	268.89° E	320 × 3810	25	25	6	1
I05721003[a]	95	−44.83°	270.02° E	320 × 2848	30	30	4	0
I05746003[a]	95	−45.21°	268.97° E	320 × 7184	26	26	4	2
MI40S087[b]	231	−40.00°	87.00° W	1016 × 1280	16	16	11	6
MI40S092[b]	231	−40.00°	92.00° W	1016 × 1280	7	7	7	7
MI45S087[b]	231	−45.00°	87.00° W	1016 × 1280	9	9	5	1
MI45S092[b]	231	−45.00°	92.00° W	1016 × 1280	10	10	10	1
V08018005[a]	17	−39.04°	268.18° E	1392 × 3270	137	2	0	0

[a] Themis image.
[b] Viking mosaic.

Zone F (basement)

Image	Scale (m/pixel)	Latitude	Longitude	Surface (pixels)	$n > 1$ km (per 10^3 km)	$n > 2.83$ km (per 10^3 km)	$n > 8$ km (per 10^3 km)
I01301002[a]	97	−21.64	301.40° E	320 × 7755	95	17	1
I01613002[a]	96	−17.73°	303.57° E	320 × 7184	33	13	2
I02343002[a]	96	−23.75°	301.98° E	320 × 7184	49	14	5
MI20S057[b]	231	−20.00°	57.00° W	1184 × 1280	49	40	14
MI25S057[b]	231	−25.00°	57.00° W	1184 × 1280	19	19	8
MI30S057[b]	231	−30.00°	57.00° W	1184 × 1280	20	13	1

[a] Themis image.
[b] Viking mosaic.

Zone F (cover)

Image	Scale (m/pixel)	Latitude	Longitude	Surface (pixels)	$n > 1$ km (per 10^3 km)	$n > 2.83$ km (per 10^3 km)	$n > 8$ km (per 10^3 km)
MI20S057[a]	231	−20.00°	57.00° W	1184 × 1280	12	7	1
MI25S057[a]	231	−25.00°	57.00° W	1184 × 1280	18	9	4
MI30S057[a]	231	−30.00°	57.00° W	1184 × 1280	16	8	2
I01563002[b]	96	−24.29°	304.67° E	320 × 3600	28	3	1
I04871003[b]	96	−27.34°	305.93° E	320 × 7851	76	12	4
I08228015[b]	98	−11.31°	306.94° E	320 × 3120	34	6	0
Row 9 MI20S052[a]	231	−20.00°	52.00° W	1184 × 1280	29	18	4
MI25S052[a]	231	−25.00°	52.00° W	1184 × 1280	24	15	4
MI30S052[a]	231	−30.00°	52.00° W	1184 × 1280	9	5	2

[a] Viking mosaic.
[b] Themis image.

Zone I

Image	Scale (m/pixel)	Latitude	Longitude	Surface (pixels)	$n > 1$ km (per 10^3 km)	$n > 2.83$ km (per 10^3 km)	$n > 8$ km (per 10^3 km)
I07617002[a]	96	−32.57°	313.64° E	320 × 2981	2.40	0.22	0.00
I09664004[a]	96	−37.68°	311.06° E	320 × 3213	2.50	0.75	0.25
I09926004[a]	96	−39.98°	312.90° E	320 × 2935	1.50	0.00	0.00
I10575007[a]	96	−35.18°	312.24° E	320 × 2816	1.22	0.61	0.00
I10912003[a]	96	−31.22°	311.55° E	320 × 2218	1.64	0.41	0.00

[a] Themis image.

References

Alonso, J.L., Pulgar, J.A., 2004. Estructura alpina de la Cordillera Cantábrica: Generalidades. In: Vera, J.A. (Ed.), Geología de España. IGM-SGE, Madrid, pp. 332–334.

Álvarez, J., and 24 colleagues, 2004. Estructura alpina del Antepaís Ibérico. In: Vera, J.A. (Ed.), Geología de España. IGME-SGE, Madrid, pp. 587–634.

Anderson, R.C., Dohm, J.M., Golombek, M.P., Haldemann, A.F., Franklin, B.J., Tanaka, K.L., Lias, J., Peer, B., 2001. Primary centers and secondary concentrations of tectonic activity through time in the western hemisphere of Mars. J. Geophys. Res. 106, 20563–20585.

Anderson, R.C., Dohm, J.M., Haldemann, A.F., Hare, T.M., Baker, V.R., 2004. Tectonic histories between Alba Patera and Syria Planum, Mars. Icarus 171, 31–38.

Anguita, F., Farelo, A.F., López, V., Mas, C., Muñoz, M.J., Márquez, A., Ruiz, J., 2001. Tharsis dome, Mars: New evidence for Noachian–Hesperian thick-skin and Amazonian thin-skin tectonics. J. Geophys. Res. 106, 7577–7589.

Baker, V.R., Maruyama, S., Dohm, J.M., 2002. A theory for the geological evolution of Mars and related synthesis (Geomars). Lunar Planet. Sci. XXXIII. Abstract 1586.

Baker, V.R., Dohm, J.M., Fairén, A.G., Ferré, T.P., Ferris, J.C., Miyamoto, H., Schulze-Makuch, D., 2005. Extraterrestrial hydrogeology. Hydrogeol. J. 13, 51–68.

Bandfield, J.L., Hamilton, V.E., Christensen, P.R., 2000. A global view of martian surface composition from MGS-TES. Science 287, 1626–1630.

Banerdt, W.B., Golombek, M.P., 2000. Tectonics of the Tharsis region of Mars: Insights from MGS topography and gravity. Lunar Planet. Sci. XXXI. Abstract 2038.

Bowin, C., Warsi, W., Milligan, J., 1981. Free-Air Gravity Anomaly Map of the World. Map and Chart Series MC-45. Geological Society of America, Boulder, CO.

Capote, R., Muñoz, J.A., Simón, J.L., Liesa, C.L., Arlegui, L.E., 2002. Alpine tectonics I: The Alpine system north of the Betic Cordillera. In: Gibbons, W., Moreno, T. (Eds.), The Geology of Spain. Geological Society, London, pp. 367–400.

Christensen, P.R., McSween, H.Y., Bandfield, J.L., Ruff, S.W., Rogers, A.D., Hamilton, V.E., Gorelick, N., Wyatt, M.B., Jakosky, B.M., Kieffer, H.H., Malin, M.C., Moersch, J.E., 2005. Evidence for magmatic evolution and diversity on Mars from infrared observations. Nature 436, 504–509.

Connerney, J.E., Acuña, M.H., Wasilewski, P.J., Ness, N.F., Réme, H., Mazelle, C., Vignes, D., Lin, R.P., Mitchell, D.L., Cloutier, P.A., 1999. Magnetic lineations in the ancient crust of Mars. Science 284, 794–798.

Connerney, J.E.P., Acuña, M.H., Ness, N.F., Kletetschka, G., Mitchell, D.L., Lin, R.P., Rème, H., 2005. Tectonic implications of Mars crustal magnetism. Proc. Nat. Acad. Sci. 102, 14970–14975.

Craddock, R.A., Greeley, R., Christensen, P.R., 1990. Evidence for an ancient impact basin in Daedalia Planum, Mars. J. Geophys. Res. 95, 10729–10741.

Crespo-Blanc, A., González, A., 2005. Influence of indenter geometry on arcuate fold-and-thrust wedge: Preliminary results of analogue modelling. Geogaceta 37, 11–14.

Cunningham, D., 2005. Active intracontinental transpressional mountain building in the Mongolian Altai: Defining a new class of orogen. Earth Planet. Sci. Lett. 240, 436–444.

Dahlen, F.A., Suppe, J., Davis, D., 1984. Mechanics of fold-and-thrust belts and accretionary wedges: Cohesive Coulomb theory. J. Geophys. Res. 89, 10087–10101.

DeSoto, G.E., Frey, H.V., 2005. Relative ages of the highlands, lowlands, and transition zone along a portion of the Mars crustal dichotomy from densities of visible and buried impact craters. Lunar Planet. Sci. XXXVI. Abstract 2383.

Dohm, J.M., Tanaka, K.L., 1999. Geology of the Thaumasia region, Mars: Plateau development, valley origins, and magmatic evolution. Planet. Space Sci. 47, 411–431.

Dohm, J.M., Tanaka, K.L., Hare, T.M., 2001. Geologic map of the Thaumasia region, Mars (1:5,000,000). USGS Misc. Inv. Ser. Map I-2650 (scale 1:5,000,000).

Dohm, J.M., Maruyama, S., Baker, V.R., Anderson, R.C., Ferris, J.C., Hare, T.M., 2002. Plate tectonism on early Mars: Diverse geological and geophysical evidence. Lunar Planet. Sci. XXXIII. Abstract 1639.

Fairén, A.G., Dohm, J.M., 2004. Age and origin of the lowlands of Mars. Icarus 168, 277–284.

Fairén, A.G., Ruiz, J., Anguita, F., 2002. An origin for the linear magnetic anomalies on Mars through accretion of terranes: Implications for dynamo timing. Icarus 160, 220–223.

Forsythe, R.D., Zimbelman, J.R., 1988. Is the Gordii Dorsum escarpment on Mars an exhumed transcurrent fault? Nature 336, 143–146.

Frey, H.V., 2003. Buried impact basins and the earliest history of Mars. In: 6th Int. Conf. on Mars. 3104.

Frey, H.V., 2004. A timescale for major events in early Mars crustal evolution. Lunar Planet. Sci. XXXV. Abstract 1382.

Ghosh, S.K., Mandal, N., Khan, D., Deb, S.K., 1992. Modes of superposed buckling in single layers controlled by initial tightness of early folds. J. Struct. Geol. 14, 381–394.

Hartmann, W.K., Neukum, G., 2001. Cratering chronology and the evolution of Mars. Space Sci. Rev. 96, 165–194.

Hauberg, E., Kronberg, P., 2001. Tempe Fossae, Mars: A planetary analogon to a terrestrial continental rift? J. Geophys. Res. 106, 20587–20602.

Hauber, E., Kronberg, P., 2003. The large Thaumasia Graben, Mars. Is it a rift? In: Proc. Sixth Internal. Conf. on Mars. 3081.

Hauber, E., Kronberg, P., 2005. The large Thaumasia Graben on Mars: Is it a rift? J. Geophys. Res. 110, doi:10.1029/2005JE002407. E07003.

Head, J.W., Greeley, R., Golombek, M.P., Hartmann, W.K., Hauber, E., Jaumann, R., Masson, P., Neukum, G., Nyquist, L.E., Carr, M.H., 2001. Geological processes and evolution. Space Sci. Rev. 96, 263–292.

Hood, L.L., Richmond, N.C., Pierazzo, E., Rochette, P., 2003. Distribution of crustal magnetic fields on Mars: Shock effects of basin-forming impacts. Geophys. Res. Lett. 30, 1281–1284.

Johnson, C.L., Phillips, R.J., 2005. Evolution of the Tharsis region of Mars: Insights from magnetic field observations. Earth Planet. Sci. Lett. 230, 241–254.

Maruyama, S., Dohm, J., Baker, V.R., 2001. Tharsis superplume: Why superplume? GSA Abstracts with programs, BTH 24.

McClay, K., Bonora, M., 2001. Analog models of restraining stepovers in strike-slip fault systems. Am. Assoc. Petrol. Geol. Bull. 85, 233–260.

McEwen, A.S., Malin, M.C., Carr, M.H., Hartmann, W.K., 1999. Voluminous volcanism on early Mars revealed in Valles Marineris. Nature 397, 584–586.

Mège, D., Masson, P., 1996a. Stress models for Tharsis formation, Mars. Planet. Space Sci. 44, 1471–1497.

Mège, D., Masson, P., 1996b. A plume tectonics model for the Tharsis province, Mars. Planet. Space Sci. 44, 1499–1546.

Montési, L.G., Zuber, M.T., 2001. Crustal thickness control on martian wrinkle ridge spacing. Lunar Planet. Sci. XXXI. Abstract 1879.

Mueller, K., Golombek, M., 2004. Compressional structures on Mars. Annu. Rev. Earth Planet. Sci. 32, 435–464.

Neumann, G.A., Zuber, M.T., Wieczorek, M.A., McGovern, P.J., Lemoine, F.G., Smith, D.E., 2004. Crustal structure of Mars from gravity and topography. J. Geophys. Res. 109, doi:10.1029/2004JE0022623. E08002.

Nimmo, F., Stevenson, D.J., 2000. Influence of early plate tectonics on the thermal evolution and magnetic field of Mars. J. Geophys. Res. 105, 11969–11979.

Okubo, C.H., Schultz, R.A., 2004. Mechanical stratigraphy in the western equatorial region of Mars based on thrust fault-related topography and implications for near-surface volatile reservoirs. Geol. Soc. Am. Bull. 116, 594–605.

Park, R.G., 1988. Geological Structures and Moving Plates. Blackie, Glasgow, UK.

Pérez Estaún, A., Bastida, F., Alonso, J.L., Marquínez, J., Aller, J., Álvarez, J., Marcos, A., Pulgar, J.A., 1988. A thin-skinned tectonics model for an arcuate fold and thrust belt: The Cantabrian Zone (Variscan Ibero-Armorican Arc). Tectonics 7, 517–537.

Phillips, R.J., Zuber, M.T., Solomon, S.C., Golombek, M.P., Jakosky, B.M., Banerdt, W.B., Smith, D.E., Williams, R.M., Hynek, B.M., Aharonson, O., Hauck, S.A., 2001. Ancient geodynamics and global-scale hydrology on Mars. Science 291, 2587–2591.

Plescia, J.B., Saunders, R.S., 1982. Tectonic history of the Tharsis region, Mars. J. Geophys. Res. 87, 9775–9791.

Pruis, M.J., Tanaka, K.L., 1995. The martian northern plains did not result from plate tectonics. Lunar Planet. Sci. XXXVI, 1147–1148.

Ramsay, J.G., 1967. Folding and Fracturing of Rocks. McGraw–Hill, New York. 568 pp.

Robinson, M.S., Tanaka, K.L., 1988. Stratigraphy of the Kasei Valles region, Mars. In: Tech. Rep. 88-05. Lunar Planet. Inst., Houston, pp. 106–108.

Romeo, I., Capote, R., Anguita, F., 2005. Tectonic and kinematic study of a strike-slip zone along the southern margin of Central Ovda Regio, Venus: Geodynamical implications for crustal plateaux formation and evolution. Icarus 175, 320–334.

Schultz, R.A., 2000. Localization of bedding slip and backthrusts above blind thrust faults: Keys to wrinkle ridge structure. J. Geophys. Res. 105, 12035–12052.

Schultz, R.A., Tanaka, K.L., 1994. Lithospheric-scale buckling and thrust structures on Mars: The Coprates rise and south Tharsis ridge belt. J. Geophys. Res. 99, 8371–8385.

Scott, D.H., Tanaka, K.L., 1981. Mars: A large highland volcanic province revealed by Viking images. Lunar Planet. Sci. 12B, 1449–1458.

Scott, D.H., Tanaka, K.L., 1986. Geological map of the Western Equatorial Region of Mars. 1:15M, I-1802-A, USGS.

Scott, D.H., Dohm, J.M., 1990. Chronology and global distribution of fault and ridge systems on Mars. Lunar Planet. Sci. XX, 487–501.

Sengör, A.M.C., Jones, I.C., 1975. A new interpretation of martian tectonics with special reference to Tharsis region. Geol. Soc. Am. Abstr. Progr. 7, 1264.

Simón, J.L., 2004. Superposed buckle folding in the eastern Iberian Chain, Spain. J. Struct. Geol. 26, 1447–1464.

Simón, J.L., 2005. Erosion-controlled geometry of buckle fold interference. Geology 33, 561–564.

Sleep, N.H., 1994. Martian plate tectonics. J. Geophys. Res. 99, 5639–5655.

Smith, D.E., Sjogren, W.L., Tyler, G.L., Balmino, G., Lemoine, F.G., Konopliv, A.S., 1999. The gravity field of Mars: Results from Mars Global Surveyor. Science 286, 94–97.

Solomon, S.C., Aharonson, O., Aurnou, J.M., Banerdt, W.B., Carr, M.H., Dombard, A.J., Frey, H.V., Golombek, M.P., Hauck, S.A., Head, J.W., Jakosky, B.M., Johnson, C.L., McGovern, P.J., Neumann, G.A., Phillips, R.J., Smith, D.E., Zuber, M.T., 2005. New perspectives on ancient Mars. Science 307, 1214–1220.

Spagnuolo, M.G., Dohm, J., 2004. Triggering the end of plate tectonics by forced climate changes. Workshop on martian Hemispheres, 4001.

Suárez, A., Heredia, N., López, F., Toyos, J.M., Rodríguez, L.R., Gutiérrez, G., 1991. Mapa Geológico de España, Hoja 102 (Los Barrios de Luna, 1:50,000). Instituto Geológico y Minero de España, Madrid.

Tanaka, K.L., Dohm, J.M., Lias, J.H., Hare, T.M., 1998. Erosional valleys in the Thaumasia region of Mars: Hydrothermal and seismic origins. J. Geophys. Res. 103, 31407–31419.

Watters, T.R., 1991. Origin of periodically spaced wrinkle ridges on the Tharsis Plateau of Mars. J. Geophys. Res. 96, 15599–15616.

Watters, T.R., Robinson, M.S., 1999. Lobate scarps and the martian crustal dichotomy. J. Geophys. Res. 104, 18981–18990.

Webb, B.M., Head, J.W., 2001. Noachian tectonics of Syria Planum and the Thaumasia Plateau. In: GSA Ann. Meeting, Session 132, poster BTH 22.

Webb, B.M., Head, J.W., 2002. Noachian tectonics of Syria Planum and the Thaumasia Plateau. Lunar Planet. Sci. XXXIII. Abstract 1358.

Zhong, S., Zuber, M.T., 2001. Degree-1 mantle convection and the crustal dichotomy on Mars. Earth Planet. Sci. Lett. 189, 75–84.

Zuber, M.T., 1995. Wrinkle ridges, reverse faulting and the depth penetration of lithospheric strain in Lunae Planum, Mars. Icarus 114, 80–92.

Zuber, M.T., Aist, L.L., 1990. The shallow structure of the martian lithosphere in the vicinity of the ridged plains. J. Geophys. Res. 95, 14215–14230.

Zuber, M.T., and 14 colleagues, 2000. Internal structure and early thermal evolution of Mars from Mars Global Surveyor topography and gravity. Science 287, 1788–1793.